Chromatic Dispersion Manipulation Based on Metalenses

Wenbo Zang, Quan Yuan, Run Chen, Lin Li, Tianyue Li, Xiujuan Zou, Gaige Zheng, Zhuo Chen, Shuming Wang,* Zhenlin Wang,* and Shining Zhu*

Metasurfaces are 2D metamaterials composed of subwavelength nanoantennas according to specific design. They have been utilized to precisely manipulate various parameters of light fields, such as phase, polarization, amplitude, etc., showing promising functionalities. Among all meta-devices, the metalens can be considered as the most basic and important application, given its significant advantage in integration and miniaturization compared with traditional lenses. However, the resonant dispersion of each nanoantenna in a metalens and the intrinsic chromatic dispersion of planar devices and optical materials result in a large chromatic aberration in metalenses that severely reduces the quality of their focusing and imaging. Consequently, how to effectively suppress or manipulate the chromatic aberration of metalenses has attracted worldwide attention in the last few years, leading to variety of excellent achievements promoting the development of this field. Herein, recent progress in chromatic dispersion control based on metalenses is reviewed.

1. Introduction

Over the past decade, as the 2D counterpart of artificial metamaterials, metasurfaces have demonstrated variety of excellent and exotic properties with an ultrathin thickness.[1–29] Assembled with subwavelength electromagnetic resonators (called as meta-atoms), metasurfaces are able to offer arbitrarily spatial phase discontinuity over the thin interface, introducing a new approach for wavefront control of light. By exciting the resonances in different meta-atoms, any required phase response can be produced, therefore, resonant phase control can be considered as an effective way for manipulating phase in metasurfaces. It should be noted that the resonant phase is depended on incident wavelength and can be tailored by geometrical parameters of meta-atoms, such as size and shape. Another way for phase generation and manipulation is to use geometric phase, or called Pancharatnam–Berry phase, which works under circularly polarized incidence and only depends on the orientation of meta-atoms. Independence of geometric size, optical resonance and intrinsic material dispersion is the main feature of geometric phase. According to these two principles, the wavefront of transmitted and reflected light field can be shaped by spatially modifying the meta-atoms at will, such as size, shape, and orientation across the metasurface.

On account of the flexible and versatile design of metasurfaces, a variety of promising applications have emerged, such as light beam shaping and steering,[1,30–32] polarization generation and modulation,[4,33–35] meta-holograms including large-angle holography and high dimensional holography,[36–40] nanolasers,[41–46] and other compact devices. Yu et al. first derived and experimentally confirmed the generalized Snell's laws of reflection and refraction.[47] According to this law, they observed a series of anomalous reflection and refraction phenomena: arbitrary reflection and refraction angles resulted from the phase gradient along the metasurface, and two different critical angles for total internal reflection that hang from the relative direction of the incident light with respect to the phase gradient and the critical angle at which the reflected beam decays (**Figure 1**a). Ni et al. experimentally demonstrated an invisible skin cloak using a metasurface with only 80 nm thick wrapped over an object.[48] By introducing a well arranged phase shift distribution in the metasurface, this skin cloak is able to conceal objects of any shape in 3D by completely restoring the phase of the reflected light at a wavelength of 730 nm (Figure 1b). Utilizing the geometric phase, Huang et al. proposed and demonstrated an effective way to handle various images with multiple recording channels via a simplified synthetic spectra holographic algorithm (Figure 1c).[49] By employing the field-effect gating realized by combining single-layer graphene with a Fano-resonant matesurface, Dabidian et al. have experimentally presented an interferometry with nanometer-scale resolution (Figure 1d).[50] Wu et al. numerically and experimentally demonstrated a metasurface polarization generator with aluminum (Al) meta-atoms, which converts linearly polarized light into six polarization

W. B. Zang, Q. Yuan, R. Chen, L. Li, T. Y. Li, X. J. Zou, Prof. G. G. Zheng,
Prof. Z. Chen, Prof. S. M. Wang, Prof. Z. L. Wang, Prof. S. N. Zhu
National Laboratory of Solid State Microstructures
School of Physics
College of Engineering and Applied Sciences
Nanjing University
Nanjing 210093, China
E-mail: wangshuming@nju.edu.cn; zlwang@nju.edu.cn;
zhusn@nju.edu.cn
W. B. Zang, Q. Yuan, R. Chen, L. Li, T. Y. Li, X. J. Zou, Prof. G. G. Zheng,
Prof. Z. Chen, Prof. S. M. Wang, Prof. Z. L. Wang, Prof. S. N. Zhu
Collaborative Innovation Center of Advanced Microstructures
Nanjing University
Nanjing 210093, China
Prof. S. M. Wang, Prof. S. N. Zhu
Key Laboratory of Intelligent Optical Sensing and Manipulation
Ministry of Education
Nanjing 210093, China

**ADVANCED
SCIENCE NEWS**

www.advancedsciencenews.com

**ADVANCED
MATERIALS**

www.advmat.de

states in visible region (Figure 1e).[51] Beside of the classical optical effects, metasurfaces also present light field manipulation in nonclassical region. Stav et al. showed the generation of four Bell states resulting from the spin–orbit coupling of photon using the geometric phase metasurface. The nonlocal correlation between two photons was consequently observed via interacting with the metasurface.[52] These results indicate that metasurfaces have the capability for generation and manipulation of entangled photon states (Figure 1f). In addition, compared to 3D structures, metasurfaces is able to relax or complete overcoming of the phase-matching requirement, which is of vital importance for nonlinear effects. Thus, metasurfaces have also been used for nonlinear optics applications, such as nonlinear generations (e.g., second harmonic generation, third harmonic generation, four-wave mixing, and high harmonic generation) enhancement,[53–59] optical meta-mixer,[60] beam deflection,[61–64] nonlinear metalenses,[61,62,65] nonlinear meta-holograms,[66,67] nonlinear polarization manipulation,[68] and beam shaping.[69]

Among all these promising applications based on metasurfaces, metasurface lens (metalens) is undoubtedly one of the most basic and important issues. By accurately producing a hyperbolic phase profile from meta-atoms with thicknesses at the wavelength scale or below, metasurfaces can be used as a lens that converges the incident light beam and even realize optical imaging. Compared to conventional bulky lenses, which precisely rely on the polished surface profiles on the transparent optical materials to achieve the desired gradual phase distributions, metalens can focus the incident light with an obviously more compact size. Different kinds of metalenses have been demonstrated with outstanding functionalities. In 2016, Capasso and co-workers first employed high-aspect-ratio titanium dioxide nanopillars to compose a millimeter-scale metalens using geometric phase. This metalens presented a numerical aperture (NA) value as high as 0.8, and achieved a diffraction-limited focusing at wavelengths of 405, 532, and 660 nm with high efficiencies of 86%, 73%, and 66%, respectively. The metalenses can resolve nanoscale features separated by subwavelength distances with image qualities comparable to a state-of-the-art commercial objective, leading to the worldwide attention on metalenses for high quality focusing and imaging (Figure 1g).[5] Straightforwardly, metalens with ultra-high NA value reach to a NA of 0.99 has also been illustrated, proving their outstanding performance for extremely optical applications (Figure 1h).[70] Combining with the micro-electromechanical systems, a tunable metalens set with one metalens movable can present accurate focal length controlling (Figure 1i).[71] Instead of one single-layered metalens, Faraon and co-workers have designed a compact doublet metalens by patterning two metasurfaces on both sides of a substrate which overcomes the aberrations of coma in imaging (Figure 1j).[72] After that, Capasso and co-workers also showed a doublet metalenses-based camera with effective off-axis coma suppressed in visible range (Figure 1k).[73] Conformal metalens covered on cylindrical lenses can be transformed to work as aspherical lenses focusing light to a point. This design achieves precisely optical aberrations correction introduced by arbitrarily shaped objects (Figure 1l).[74] By using metalens as part of the immersion objectives, Chen et al. demonstrated liquid immersion focusing

Wenbo Zang received her B.S. degree in physics from Nanjing University, China in 2016. She is now a Ph.D. student in optics at National Laboratory of Solid State Microstructures and School of Physics in Nanjing University. She is engaged in simulation, experiment, and nanofabrication related to nanophotonics based on metamaterials. Her current research interests are nonlinear optics, quantum photonics, metasurfaces, and their applications.

Shuming Wang received his Ph.D. degree in physics from Nanjing University, China in 2009. He is an associate professor at the National Laboratory of Solid State Microstructures, School of Physics, Nanjing University, specializing in nanophotonics, metasurfaces (metamaterials), plasmonics, and quantum optics.

free of spherical aberration at various design wavelengths in the visible spectrum (Figure 1m).[75]

Attributed to intrinsic dispersion in used materials and high resonant phase dispersion of meta-atoms, metasurfaces significantly exhibit large chromatic dispersion. On the one hand, although metalenses show excellent optical functionalities and allow much more compact design than the conventional high-end objective lenses, chromatic aberration in the metalenses strongly restrict their further applications, which was already pointed out in the milestone work of metalens with large diameter, high efficiency and high NA value.[5] Eliminating the chromatic aberration over a continuous wavelength region is particularly important in some colorful imaging devices. On the other hand, the large chromatic dispersion with intelligent design in metasurfaces can be utilized to realize or optimize some specific optical devices, such as spectrometer, nano-optic endoscope, full-color router and multiwavelength holograms. Comparing with conventional optics, the utilization of metasurfaces have great advantages in the development of compact and integrated optical devices with complex functions. So there is growing concern about the control of chromatic dispersion. Here, we highlight the noticeable achievements over the past few years in the field of chromatic aberration control and in the development of achromatic lenses as well as attempt to provide our perspective on this specific branch of applications. The rest of this paper is organized in the following sections. In Section 2, we briefly explain chromatic aberration. Sections 3–5 are devoted to the working mechanisms and demonstrations
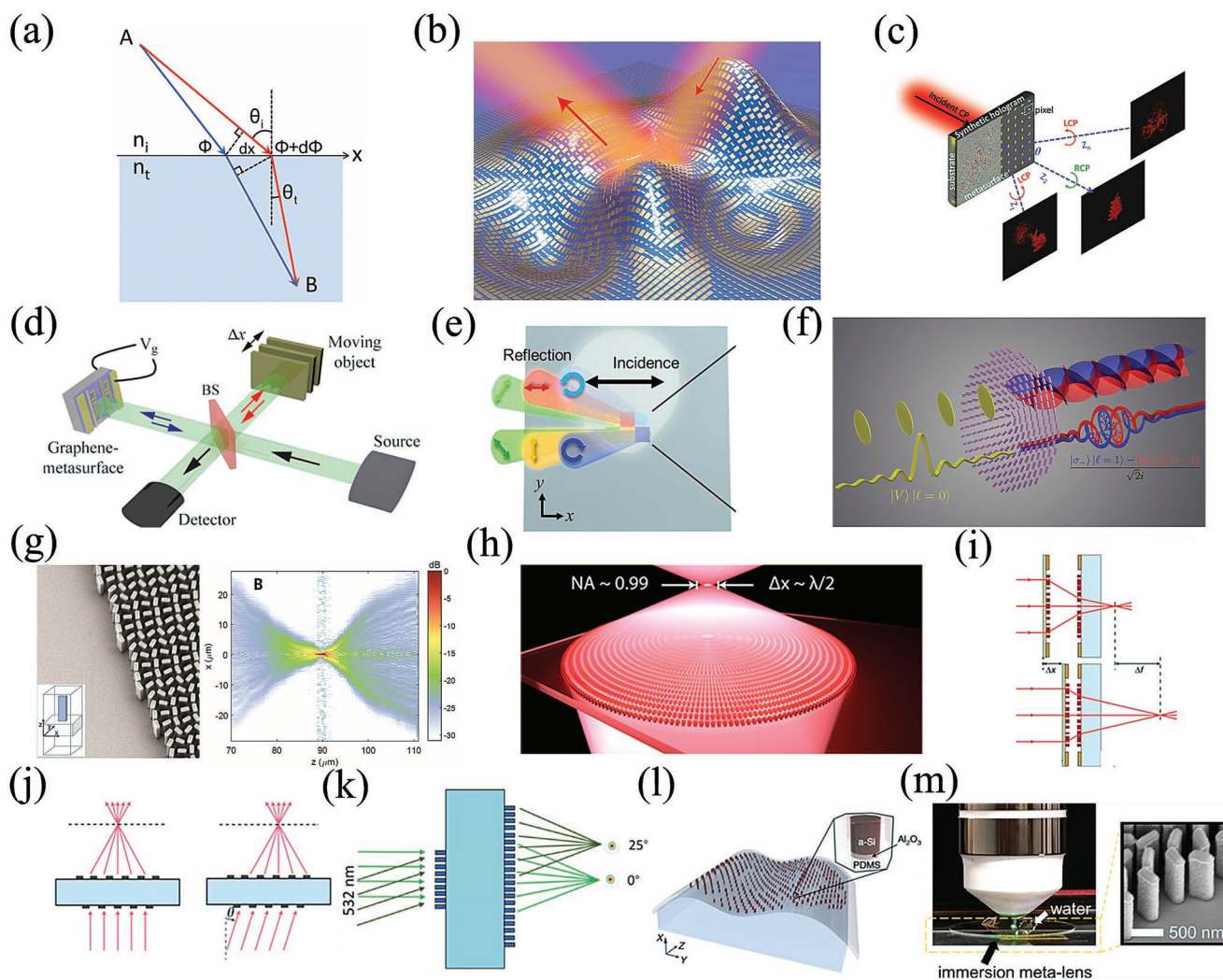
**ADVANCED
SCIENCE NEWS**

www.advancedsciencenews.com

**ADVANCED
MATERIALS**

www.advmat.de

Figure 1. a) The schematics used to derive the generalized Snell's law of refraction. b) A 3D illustration of a metasurface skin cloak. c) Schematic illustration of the hybrid multiplexing with a plasmonic metasurface. d) Schematic of the interferometric motion detection using a graphene-integrated metasurface. e) Schematic of polarization conversion with Al plasmonic metasurfaces for arbitrary polarization generation with fixed incident polarization. f) Schematic of entanglement between spin and orbital angular momentum on a single photon through a metasurface. g) A metalens with a NA of 0.8 composed of high-aspect-ratio nanopillars. h) Schematic of a metalens with ultrahigh NA value of 0.99. i) Schematic of a tunable metalens which can control accurate focal length. j) A compact doublet metalens overcoming the aberrations of coma in imaging. k) A doublet metalenses-based camera with great off-axis. l) Schematic of optical aberrations correction introduced by arbitrarily shaped objects. m) A liquid immersion metalens focusing free of spherical aberration. a) Reproduced with permission.[47] Copyright 2011, American Association for the Advancement of Science. b) Reproduced with permission.[48] Copyright 2015, American Association for the Advancement of Science. c) Reproduced with permission.[49] Copyright 2015, Wiley-VCH. d) Reproduced with permission.[50] Copyright 2016, American Chemical Society. e) Reproduced with permission.[51] Copyright 2017, American Chemical Society. f) Reproduced with permission.[52] Copyright 2018, American Association for the Advancement of Science. g) Reproduced with permission.[5] Copyright 2016, American Association for the Advancement of Science. h) Reproduced with permission.[70] Copyright 2018, American Chemical Society. i) Reproduced under the terms of the CC-BY Creative Commons Attribution 4.0 International License (http://creativecommons.org/licenses/by/4.0/).[71] Copyright 2018, The Authors, published by Springer Nature. j) Reproduced under the terms of the CC-BY Creative Commons Attribution 4.0 International License (http://creativecommons.org/licenses/by/4.0/).[72] Copyright 2016, The Authors, published by Springer Nature. k) Reproduced with permission.[73] Copyright 2017, American Chemical Society. l) Reproduced under the terms of the CC-BY Creative Commons Attribution 4.0 International License (http://creativecommons.org/licenses/by/4.0/).[74] Copyright 2016, Springer Nature. m) Reproduced with permission.[75] Copyright 2017, American Chemical Society.

of multiwavelength, narrowband, and broadband achromatic, respectively. Other chromatic applications including spectroscopy, endoscopic imaging, color router, and color holograms will be reviewed in Section 6. Finally, we summarize and provide perspective for future developments in Section 7.

2. The Description of Chromatic Dispersion

Chromatic dispersion is one of the key characteristics of optical materials, which always plays a critical role in designing optical components and systems. Traditional refractive optics relies on the gradual phase accumulation through propagation. In

materials with normal chromatic dispersion like glasses, the index of refraction decreases with the longer wavelength so that such kind of refractive lenses have larger focal distances and prisms deflect at a smaller angle in red than in blue. On the other hand, operated by means of interference of light transmitted through an amplitude or phase mask, diffractive optical elements exhibit opposite chromatic aberration. The focal length is shorter and deflection angle is bigger corresponds to a longer wavelength.[76] Complete elimination of chromatic aberration can be accomplished by integrating several materials with complementary dispersion into a single component to obtain the same focal length for multiple wavelengths, as in an achromatic doublet and triplet.[77] However, this strategy adds weight, complexity, and cost to optical imaging systems, which greatly limits their usage.

With a specially designed arrangement of meta-atoms, metasurfaces can locally impart abrupt phase shift to purposely manipulate the scattered wavefront at will, which provides a new mechanism for light control. The total accumulated phase for a converting metalens is the sum of two parts: the phase shift imparted by the metalens and the phase accumulated via propagation through free space. To convert incident planar wavefront, the typical distribution of phase retardation for a metalens should be[78]

$$\varphi\left(R,\lambda\right) = -\left[2\pi\left(\sqrt{R^2 + f^2} - f\right)\right]\frac{1}{\lambda} \tag{1}$$

where $R = \sqrt{x_0^2 + y_0^2}$ is the distances from arbitrary position (x_0, y_0) on the metalens surface to the center and f is the focal length. Apparently, there are two variables in the function of required phase that leads to great difficulty in realizing the exact phase at different wavelength at every position of the lens. The traditional treatment by combining different lenses with different chromatic dispersions can successfully cancel the chromatic aberration at several wavelength leading to an approximate achromatic effect over a relatively broad bandwidth. However, such treatment does not provide two independent degrees of freedom to manage the two-parameter phase in Equation (1), thus the perfect achromatism cannot be achieved via traditional approach in principle.

3. Multiwavelength Achromatic Metalenses

Up to now, many groups proposed the multiwavelength achromatic metalens in the visible spectrum range using dispersion engineering of the nanostructure, aiming at improving the lens' performance of a set of discrete wavelengths. Several mechanisms of compound metalenses in cascading or spatially composed of diverse configurations designed for different working wavelengths have been proved to be feasible. Different from traditional optical lenses, metalenses do not need to introduce new material components to achieve achromatism and other functions, which leads the way to realize integration and miniaturization of optical devices. In order to realize a triply achromatic metalens, for blue (450 nm), green (550 nm), and red (650 nm) light, Avayu et al. utilized stacked multilayered metasurfaces to demonstrate functional spectral multiplexing

of broadband visible light which is conceptually simple but effective.[79] The multilayered metalens consist of three-layer closely stacked metallic disc-shaped nanoparticles made of different materials: Al for blue light, silver (Ag) for green light and gold (Au) for red light (The schematic illustrations of the three-layer lens and the layered metallic nanodiscs are shown in the left column of **Figure 2**a). The parametric tunable polarization-independent nanodiscs are optimized to support localized surface plasmon resonances at wavelengths of 450, 550, and 650 nm of the visible spectrum, respectively. Each plasmonic metasurface is composed of corresponding nanodiscs arranged for a narrow band binary Fresnel zone plate lenses and focuses its targeted part of the visible spectrum to the same distance of 1 mm along the optical axis. The right column of Figure 2a shows the measured light focusing effect with conventional Fresnel zone plate lens and multilayered achromatic metalens under white illumination and color imaging using the metalens, respectively, which illustrate the ability of chromatic aberration correction of this approach. The distance among different nanodiscs in a same layer is very close to avoid diffraction-grating effects and a distance of 200 nm between layers is chosen to minimize near-field crosstalk among the individual nanodiscs in different layers so that each one operates independently. This creative multilayer design concept realized the first chromatically corrected metasurface triplet lens with complex functionalities for red, green, and blue (RGB) colors but the measured focusing transmission efficiency in the range of 5.8–8.7% is not high because of metal loss and fabrication limitations. Low efficiency and fabrication difficulty with extra alignment still limit its broader applications. Lin et al. constructed interleaved Si-based metasurfaces that can realize axial and lateral focus of three primary RGB wavelengths (480, 550, and 620 nm).[80] The composite metasurfaces are composed of the complementary sub-elements divided from three original lenses, which respectively focus red, green or blue to the same focal plane by the control of geometric phase. The illustration of the approach to construct interleaved multiwavelength achromatic metasurfaces and its focusing effect as well as color imaging are shown in Figure 2b. In previous works, Faraon and co-workers used amorphous silicon nanoposts to realize polarization-insensitive high-contrast transmission metalenses with very high efficiencies including high NA lenses, simultaneous phase and polarization controllers and wide-angle miniature optical planar camera, which have single operation wavelength in common.[72,81,82] In their later research, they demonstrated high contrast dielectric polarization insensitive metalenses with amorphous silicon nanoposts that focus light at 915 and 1550 nm to the same focal distance.[83] The two different double-wavelength metalenses based on large scale segmentation and meta-atom interleaving are investigated, respectively, as shown in Figure 2c. Though efficiencies of the multisector device at the two wavelengths are closer to each other than the interleaved lens, the multiple macroscopic sectors changes the shape of its focal spot while the interleaved design does not cause this issue. Due to the weak coupling the nanoposts behave like individual scatterers with large cross-section, and thus a unit cell consisting of multiple meta-atoms, called meta-molecules, can be chosen for the optimal design. The same research group utilized meta-molecules with four different nanoposts, which has
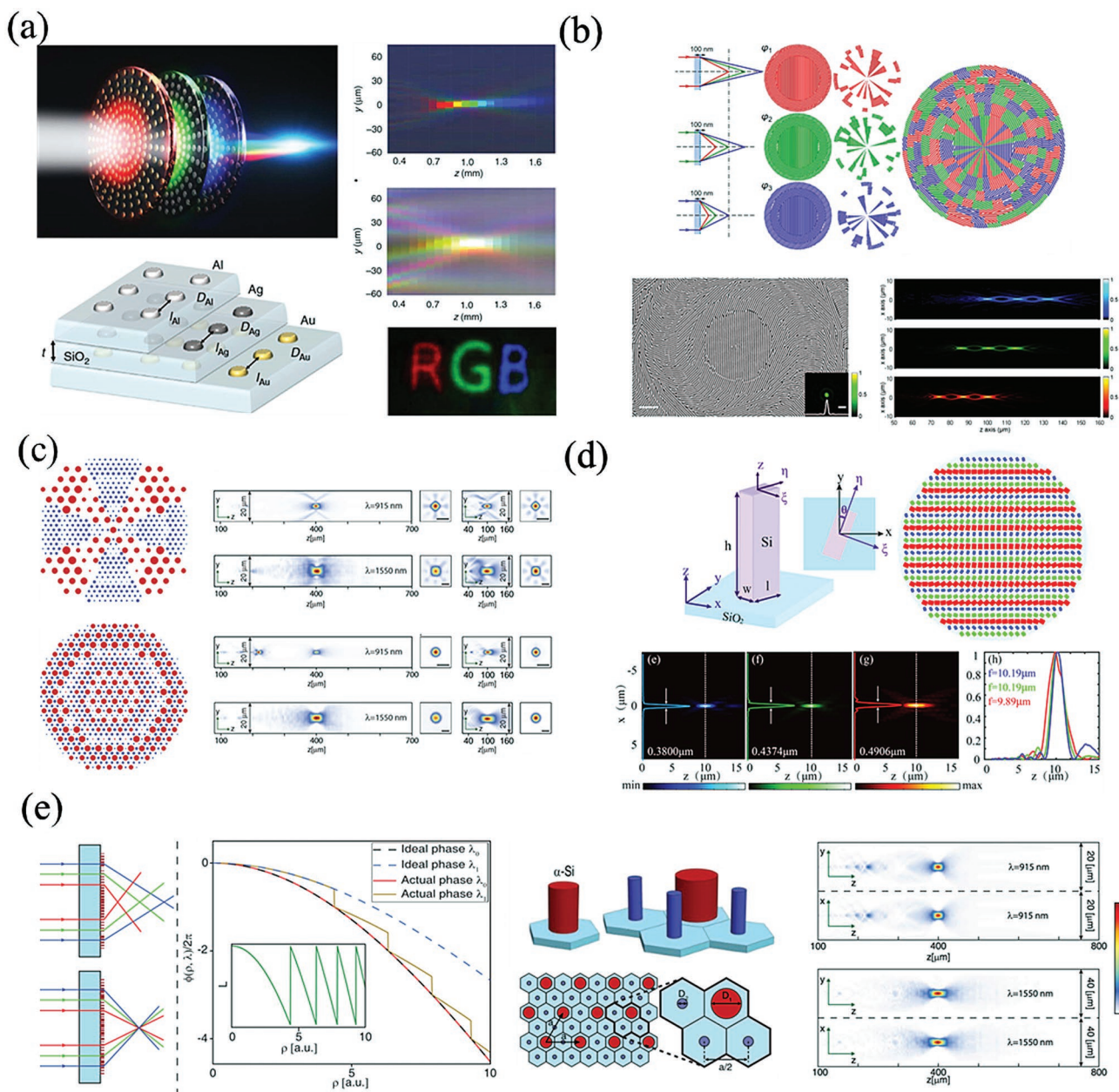
Figure 2. a) A vertical stacking metalenses made of three different metallic nanodiscs shows the same focal distance at red, green, and blue light. b) A composite metalens consisting of three randomly segmented Si-based sublenses achieves light focusing at three primary red, green, and blue wavelengths to the same focal length. c) Polarization insensitive metalenses comprised of nanoposts in multisector lens (upper panel) and interleaved lens (lower panel). d) A compound metalens comprised of discrete wavelengths manipulating nanopillars achieves light focusing at three primary red, green, and blue wavelengths to the same focal length. e) Multiwavelength polarization-insensitive metalenses with meta-molecules. a) Reproduced under the terms of the CC-BY Creative Commons Attribution 4.0 International License (http://creativecommons.org/licenses/by/4.0/).[79] Copyright 2017, The Authors, published by Springer Nature. b) Reproduced with permission.[80] Copyright 2016, American Chemical Society. c) Reproduced under the terms of the CC-BY Creative Commons Attribution 4.0 International License (http://creativecommons.org/licenses/by/4.0/).[83] Copyright 2016, The Authors, published by Springer Nature. d) Reproduced with permission.[85] Copyright 2017, Optical Society of America. e) Reproduced with permission.[84] Copyright 2016, Optical Society of America.

more parameters to independently control the phases at different wavelengths, to realize simultaneously focus at 915 and 1550 nm (Figure 2e).[84] The double-wavelength aspherical lens has efficiencies of 22% and 65% at 915 and 1550 nm, respectively, for NA = 0.46. Li et al. designed a spatial multiplexing dielectric achromatic metalens which realize focus of three

wavelengths at visible frequency (473, 532, and 632.8 nm).[85] The concept of spatial multiplexing is adopted for three dedicatedly designed silicon nanocuboids corresponding to the three specific wavelengths, respectively. With geometric phase, the chromatic dispersion among different wavelengths can be engineered independently (Figure 2d).

Different from the above mentioned multiwavelength metalenses based on combining several metalenses designed for special frequencies into one, single metalens version based on new design principles have also been demonstrated. After proper design, meta-atoms can provide desired phase at different wavelengths. Capasso's group demonstrated a meta lens without chromatic aberrations at three wavelengths (1300, 1550, and 1800 nm) based on low-loss dielectric resonators, which introduce a dense spectrum of optical modes to enable dispersive phase compensation.[76] Multiple resonances of coupled rectangular dielectric resonators are used as building blocks to provide the phase coverage at the three wavelengths. The achromatic metalens presents good focusing at the focusing distance of 7.5 mm at the three wavelengths (1300, 1550, and 1800 nm) can be theoretically designed (see in **Figure 3**a). Accordingly, utilizing the aperiodic array of
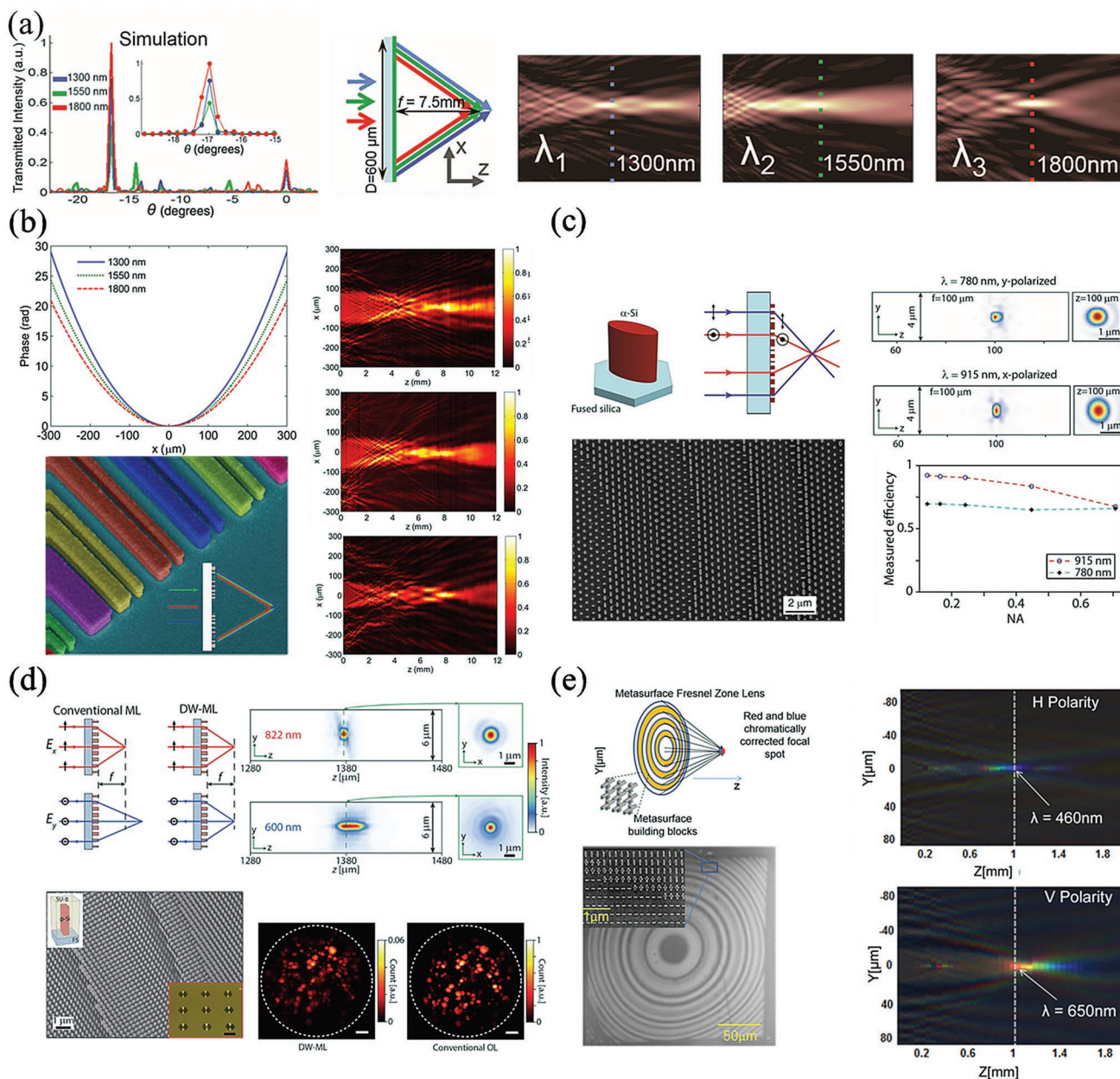

Figure 3. a) Multiwavelength achromatic metalenses by dispersive phase compensation of 1300, 1550, and 1800 nm wavelengths. b) Metasurfaces consisting of coupled rectangular Si resonators focus three wavelengths of 1300, 1550, and 1800 nm to the same line. c) Double-wavelength metalenses designed with birefringent elliptical meta-atoms. d) Two-photon microscopy with a double-wavelength metalens based on polarization manipulating. e) Diffractive metasurface based FZP that corrects chromatic aberrations at pairs of wavelengths by polarization controlling. a) Reproduced with permission.[76] Copyright 2015, American Association for the Advancement of Science. b) Reproduced with permission.[86] Copyright 2015, American Chemical Society. c) Reproduced with permission.[87] Copyright 2016, Optical Society of America. d) Reproduced with permission.[88] Copyright 2018, American Chemical Society. e) Reproduced with permission.[89] Copyright 2015, Optical Society of America.

ADVANCED
SCIENCE NEWS
www.advancedsciencenews.com

ADVANCED
MATERIALS
www.advmat.de

coupled dielectric nanoresonators, they experimentally demonstrated the achromatic metalens at three wavelengths with the focal efficiencies being 15%, 10%, and 21%, respectively and the focal spot close to the diffraction limit for a NA of 0.05 (see in Figure 3b).[86] Then, they also demonstrated a metasurface able to deflect three wavelengths at the same angle of 17° with the efficiency of 9.8%, 10.3%, and 12.6%, respectively. This multiwavelength achromatic demonstration is a significant step toward the realization of achromatic optical devices, but a generalized approach to make the phase shift distribution satisfying a wavelength-dependent function was not provided for achromatic metalenses requiring more wavelengths or even broad bandwidth. Besides, based on the anisotropic property of amorphous silicon nanoposts with elliptical cross sections, Faraon and co-workers demonstrated double-wavelength metalenses those focus light at 780 and 915 nm with perpendicular linear polarizations to the same position.[87] The anisotropic nanoposts have two independent parameters, the two cross diameters of the elliptical cross sections, those are utilized to control the phase of lights with two different wavelengths and orthogonal polarizations. The birefringent metalenses with efficiencies from 65% to above 90% and NA up to 0.7 are demonstrated at both wavelengths. The elliptical meta-atom with birefringence, scanning electron microscopy (SEM) image, and focusing effect are shown in Figure 3c. The similar birefringent dichroic polycrystalline silicon nanoposts with asymmetric rectangular cross sections were used to independently control the phase of two orthogonal polarizations at 820 and 605 nm, corresponding to the excitation and emission wavelengths of the measured fluorophores.[88] Light with two different wavelengths are focused to the same plane for two-photo microscopy and its image quality are comparable to a conventional microscope objective, as shown in Figure 3d. The focusing efficiencies of the double wavelength metalens were measured to be 61% and 27% at 822 and 600 nm with a NA of 0.5. Though this approach is powerful and efficient for double-wavelength achromatic metalenses even multiwavelength combined with met-molecule concept, this dichroic birefringent principle makes effective achromatism unable to have broad working wavelengths and requires lights with different wavelengths to have special polarizations, which greatly limit its applications. Similarly, Eisenbach et al. demonstrated designed diffractive Fresnel zone plate lenses that focus blue (460 nm) and red (650 nm) lights with two orthogonal polarizations to the same focal point.[89] The metalenses are composed of tightly packed cross and rod shaped optical nanoantennas with strong polarization and wavelength selectivity. Figure 3e shows the schematic diagram, SEM and focusing effects at two working wavelengths of this metasurface Fresnel zone lens.

Topology optimization is another effective method for multiwavelength achromatic metalenses. Diffractive optics can readily enable broadband focusing, while still maintaining the planar architecture. Wang et al. designed chromatic-corrected diffractive metalenses composed of pixelated, multilevel squares (2D) and linear grooves (1D).[90] With fixed width dictated by the resolution of fabrication, each groove with specific height imparts a relative phase shift, which is related with wavelength, position and height of the groove. The distribution of groove heights is optimized by a modified direct-binary-search algorithm, which is a generally applicable perturbation-based iterative method for super-achromatic performance. The demonstrated diffractive lens with different numbers of grooves and focal lengths are all able to focus the three discrete wavelengths (460, 540, and 620 nm) to the same point in space with average measured efficiencies of 24.9%, 23.0%, and 21.5% (**Figure 4**a). This optimization algorithm is effective in eliminating chromatic aberration for multiwavelength diffractive optics. Although the devices demonstrated in this work is 1D, they can be readily extended to 2D and also applicable to almost any electromagnetic spectrum and arbitrary optical parameters that benefited from the high design flexibility and generality. In addition, this one-step grayscale lithography makes it easy and cheap to fabricate and replicate these large size optical devices. Hu et al. described an evolutionary approach to design flat multiwavelength achromatic lenses over the visible to near-infrared wavelength range based on subwavelength plasmonic multiple nanoparticles with different sizes and shapes.[91] The lattice evolution algorithm used finite-difference time-domain simulations to calculate the optical fields from each nanoparticle and realized achromatic lattice lenses at three wavelengths (600, 785, and 980 nm) by tuning the arrangement of the phase units on a discrete square lattice. The schematic diagram of this plasmonic lattice lens and its multiwavelength achromatic focusing images are set in Figure 4b. Compared with nanohole elements in their previous work,[92] nanoparticles lattice lenses have higher transmission efficiencies while maintaining the same focusing accuracy. Based on the multiobjective optimization capabilities of the algorithm, the working wavelengths of these achromatic lenses can be extended to deep ultraviolet to visible range (200–500 nm) under the replacement of plasmonic materials and even in a broadband spectrum. It can be predicted that the evolutionary-algorithm approach of nanostructure design will lead to the development of many fields, such as integrated optoelectronics, miniaturized optical interconnects, high-resolution optical microscopy and so on. However, these optimization approaches only provide the design approximate to multiwavelength or broadband achromatism but do not solve the problem of chromatic aberration of metalenses in principle yet. So the focusing efficiency of algorithm-optimized lenses is not high even if low-loss dielectric materials are used. The essence of holographic phase coding can be resorted to multiwavelength chromatic aberration elimination and even arbitrary multispectral beam manipulation. Zhao et al. encoded the geometric phase information of different wavelengths into single multispectral metasurface based on the spin–orbit interaction in nanoaperture array.[93] Due to the broadband property of the spin–orbit interaction, the designed metasurface can realize arbitrary-shaped focal spots at discrete wavelengths and exhibit unvaried focal length at wavelengths of 532, 632.8, and 785 nm (see in Figure 4c).

4. Narrowband Achromatic Metalenses

With increasing number (or bandwidth) of the working wavelengths, the design complexity of achromatic metalenses increases dramatically. At the same time, the adverse coupling and interference between meta-atoms greatly limit the
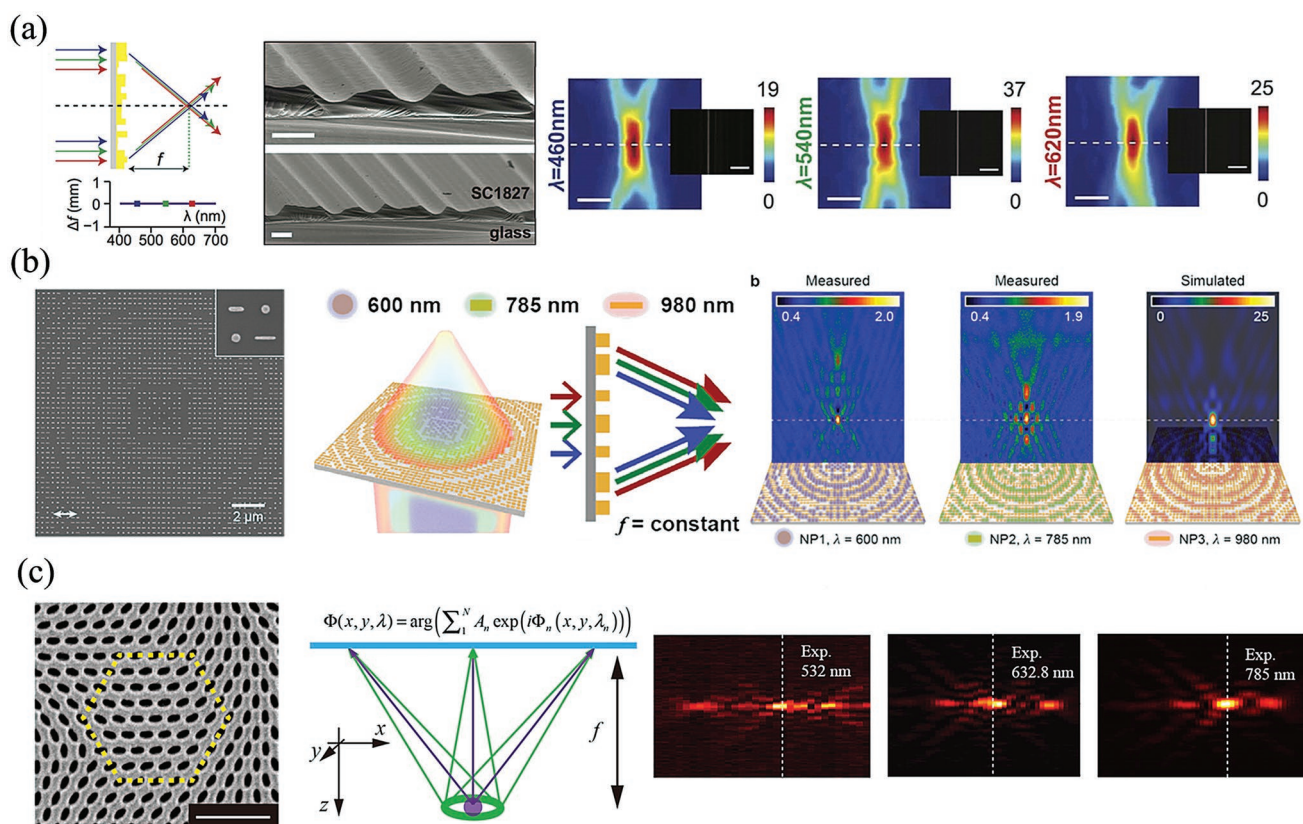
Figure 4. a) Three-wavelength apochromatic diffractive lenses. b) Multiwavelength achromatic lenses based on subwavelength plasmonic nanoparticles using lattice evolution algorithm. c) Multispectral achromatic metalenses by encoded phase information. a) Reproduced under the terms of the CC-BY Creative Commons Attribution 4.0 International License (http://creativecommons.org/licenses/by/4.0/).[90] Copyright 2016, Springer Nature. b) Reproduced with permission.[91] Copyright 2016, American Chemical Society. c) Reproduced under the terms of the CC-BY Creative Commons Attribution 4.0 International License (http://creativecommons.org/licenses/by/4.0/).[93] Copyright 2015, Springer Nature.

applicability and effectiveness of metalenses. New approach or mechanism is urgently needed for the development of broadband achromatic metasurfaces.

In order to make full use of the advantages of large amplitude and wide phase coverage of metal mirrors, several experiments were carried out using the reflection version. Capasso and his collaborators used titanium dioxide (TiO$_2$) nanopillars with square cross-section on a metallic mirror with a thin layer of silicon dioxide (SiO$_2$) in-between to demonstrate an achromatic reflective metalens operating over a narrowband in visible.[94] There are two advantages for choosing square cross-section: first, it increases the phase coverage with maximizing the filling factor from 0 to 1; second, it results in a polarization insensitive design. Their calculation results on phase shift as a function of the nanopillar width at wavelengths of interest shows that several choices of widths can provide the same phase but different dispersive values at specific wavelength simultaneously. Originating from the excitation of guided mode resonances the unfolded phase shift is a nonmonotone function of the nanopillar width, which provides another degree of freedom to control the chromatic dispersion. In addition, since the phase at the referenced lens center have distinct values for different wavelengths which can be used as a free parameter, they utilized optimization algorithm to minimize the difference between the implemented and required phase simultaneously

for all wavelengths. Finally they experimentally achieved an achromatic metalens with a NA of 0.2 and a constant focal length over a continuous 60 nm range of wavelengths from 490 to 550 nm. Schematic of the achromatic metalens and its TiO$_2$ nanopillar building block, phase shift as a function of the nanopillar width and measured focusing effect at different wavelengths are shown in **Figure 5**a, respectively. Moreover, a metalens with reverse chromatic dispersion was also demonstrated which further proved the effectiveness of this approach to realize metalenses with tailored chromatic dispersion.

With the similar design principle, Faraon and co-workers demonstrated narrowband dielectric focusing mirrors with positive, zero and hyper-negative dispersion in infrared.[95] The reflective metasurface is composed of square cross-section amorphous silicon nanoposts on a low refractive index SiO$_2$ spacer layer on an Al reflector, which were used to provide 0–2π phase coverage and different phase dispersions. The achromatic metalens exhibits a highly diminished chromatic dispersion in the wavelength range of 1450–1590 nm and maintains efficiency around 50% in the whole working spectra. Figure 5b shows SEM image of the fabricated metalens, schematic of the square cross-section nanopost meta-atom and measured intensity distributions of the achromatic metalens at five wavelengths, respectively. On the other hand, the demonstration of the hyper-positive and hyper-negative dispersion metalenses
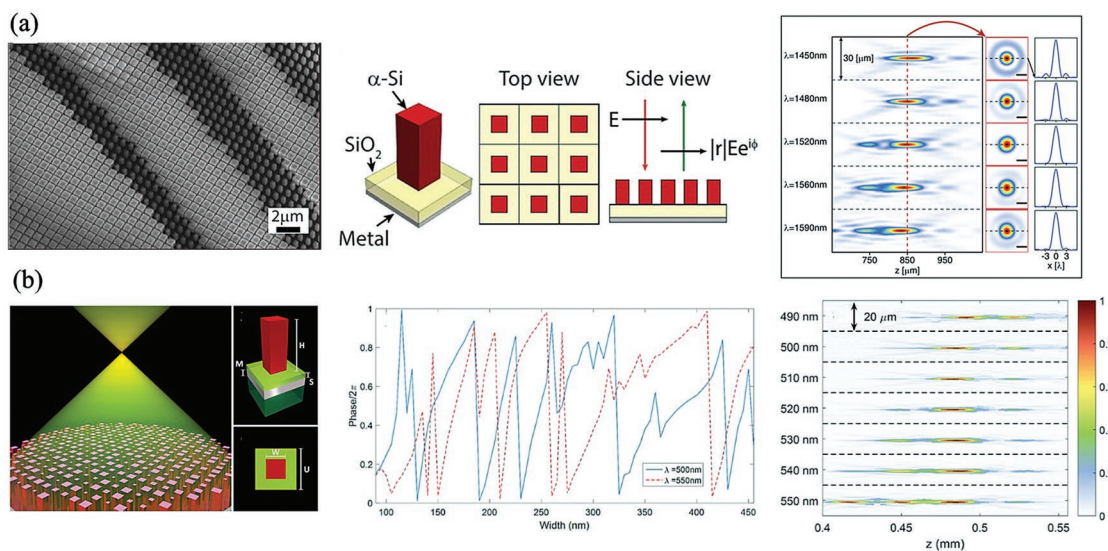
**ADVANCED
SCIENCE NEWS**

www.advancedsciencenews.com

**ADVANCED
MATERIALS**

www.advmat.de

Figure 5. Narrowband achromatic metalenses. a) Dispersion-engineered metasurfaces with positive, zero, and hypernegative dispersions. b) Building blocks made of TiO$_2$ nanopillars, a dielectric spacer, and a metallic back reflector were applied to realize an achromatic metalens with over 60 nm continuous bandwidth. a) Reproduced with permission.[94] Copyright 2017, American Chemical Society. b) Reproduced with permission.[95] Copyright 2017, Optical Society of America.

using this approach proved better that independent control over phase and dispersion of meta-atoms is an effective method of engineering the chromatic dispersion of metasurface devices over continuous wavelength regions. But it is noteworthy that in those works on narrowband achromatic metalenses mentioned above, the elimination of chromatic aberration is actually an approximation effect with optimized specific geometric parameters. That means each specific functional meatasurface for engineering the chromatic dispersion need a vast number of calculations to satisfy its corresponding phase condition. New design principle of achromatic metalens over continuous range of wavelengths remains to be proposed.

5. Broadband Achromatic Metalenses

In an early work, a broadband achromatic cylindrical lens across the visible spectrum (from 450 to 600 nm) was demonstrated through the optimization based on a modified direct-binary-search algorithm, as shown in **Figure 6**a.[90] However, it owns low efficiency and numerical aperture (NA = 0.013), restriction of the constituent materials to resists and not very ideal focusing effect greatly limit its universality and applicability. Wang et al. recently have proposed a completely new design principle to realize broadband achromatic metalenses and gradient metasurfaces, which successfully eliminates the chromatic aberration in infrared wavelength range of 1200 to 1680 nm in reflective mode for circularly-polarized incidences.[78] Phase retardation with a fixed focal length is necessary in a wide range of wavelength for a broadband achromatic metalens, so the phase in Equation (1) is divided into two components

$$\varphi(R, \lambda) = \varphi(R, \lambda_{\max}) + \Delta\varphi(R, \lambda) \qquad (2)$$

The former part in Equation (2) is considered as a basic phase profile, which is only related with $\lambda_{\max}$ (top boundary of the working wavelength band) but independent to the working wavelength λ. Such phase profile can be obtained by using geometric phase as phase modulation in each meta-atom, which is only dependent on the orientation of the resonant elements in metasurfaces illuminated by circularly polarized light. The latter part in Equation (2), linear with $1/\lambda$, is considered as the chromatic aberration phase, which can be acquired by the phase response of each ingeniously designed meta-atom. In this work, as shown in Figure 6b, they utilized a sandwich structure formed by a couple of specially Au nanorods, SiO$_2$ spacer and Au back reflector as the basic unit cell to realize smooth and linear phase compensation with working frequency. Different designs of the multiple resonances of the nanorods can provide different phase-changing slopes and adding more resonators can realize larger phase compensation. Since the geometric phase and phase compensation from integrated-resonant unit elements is completely different in mechanism, these two parts of phase won't disturb with each other, but can be simply merged together. Employing the proposed policy, broadband achromatic metalenses with NA up to 0.324 and the efficiency on the order of ≈12% are demonstrated finally. SEM image of fabricated metalens, measured and simulated focal length of broadband achromatic metalenses and their measured intensity profiles along axial planes at different wavelengths are shown in Figure 6c and obviously the focal length keeps almost unchanged. In addition, a broadband achromatic gradient metasurface is also demonstrated, further indicating the realization of a broadband achromatic converging property in near infrared. Then as with higher plasma frequency and lower loss in visible, aluminum was used into a similar design of achromatic metalenses working from 400 to 667 nm with efficiency above 20%, as shown in Figure 6d.[96]
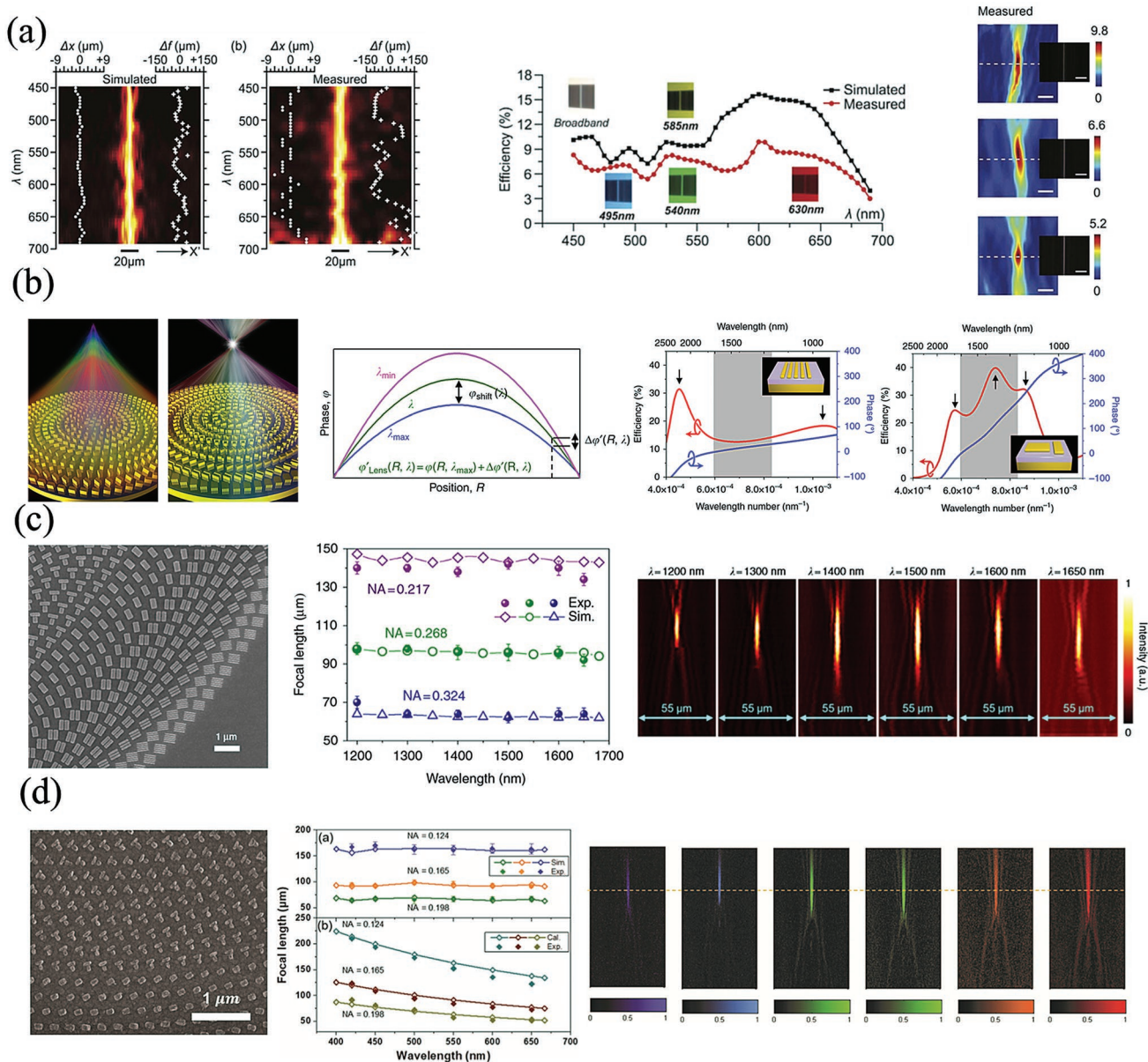
Figure 6. a) Broadband focusing onto a single line by diffractive lens for the entire visible band (450 to 700 nm). b) Au integrated-resonant unit elements and new design principle to realize broadband achromatic metalens. c) Au-IRUs metalens displaying unvaried focal distance in a broad infrared bandwidth of 1200–1680 nm. d) Visible Al-IRUs metalens achieving achromatic focusing from 400 to 667 nm. a) Reproduced under the terms of the CC-BY Creative Commons Attribution 4.0 International License (http://creativecommons.org/licenses/by/4.0/).[90] Copyright 2016, Springer Nature. b,c) Reproduced under the terms of the CC-BY Creative Commons Attribution 4.0 International License (http://creativecommons.org/licenses/by/4.0/).[78] Copyright 2017, The Authors, published by Springer Nature. d) Reproduced with permission.[96] Copyright 2018, Wiley-VCH.

As a proof-of-concept work, the demonstration of achromatic reflective metalenses in near infrared proves the effectiveness of dividing the phase into a basic phase profile and the chromatic aberration phase for broadband chromatic aberration elimination. Although reflective metalenses are useful in some cases, transmission optical devices are highly desirable in practical applications especially for metalenses working in the visible. With a similar strategy, Wang et al. used dielectric gallium nitride (GaN) integrated-resonant units to achieve a visible broadband achromatic metalens from 400 to 660 nm in transmission mode.[97] As a transparent low loss semiconductor

material with high refractive index in visible spectrum, GaN simultaneously has high hardness and physical and chemical stability as well as low-cost and semiconductor foundry compatibility so it is an ideal choice for material of the metalens. Because of the weak optical coupling among high refractive index dielectric nanostructures, together with the waveguide-like cavity multiresonances, large phase compensation can be obtained by directly increasing the thickness of the nanostructures. Wang and co-workers therefore utilized solid and inverse high-aspect ratio nanopillars with a fixed thickness of 800 nm to introduce large phase compensation, which is
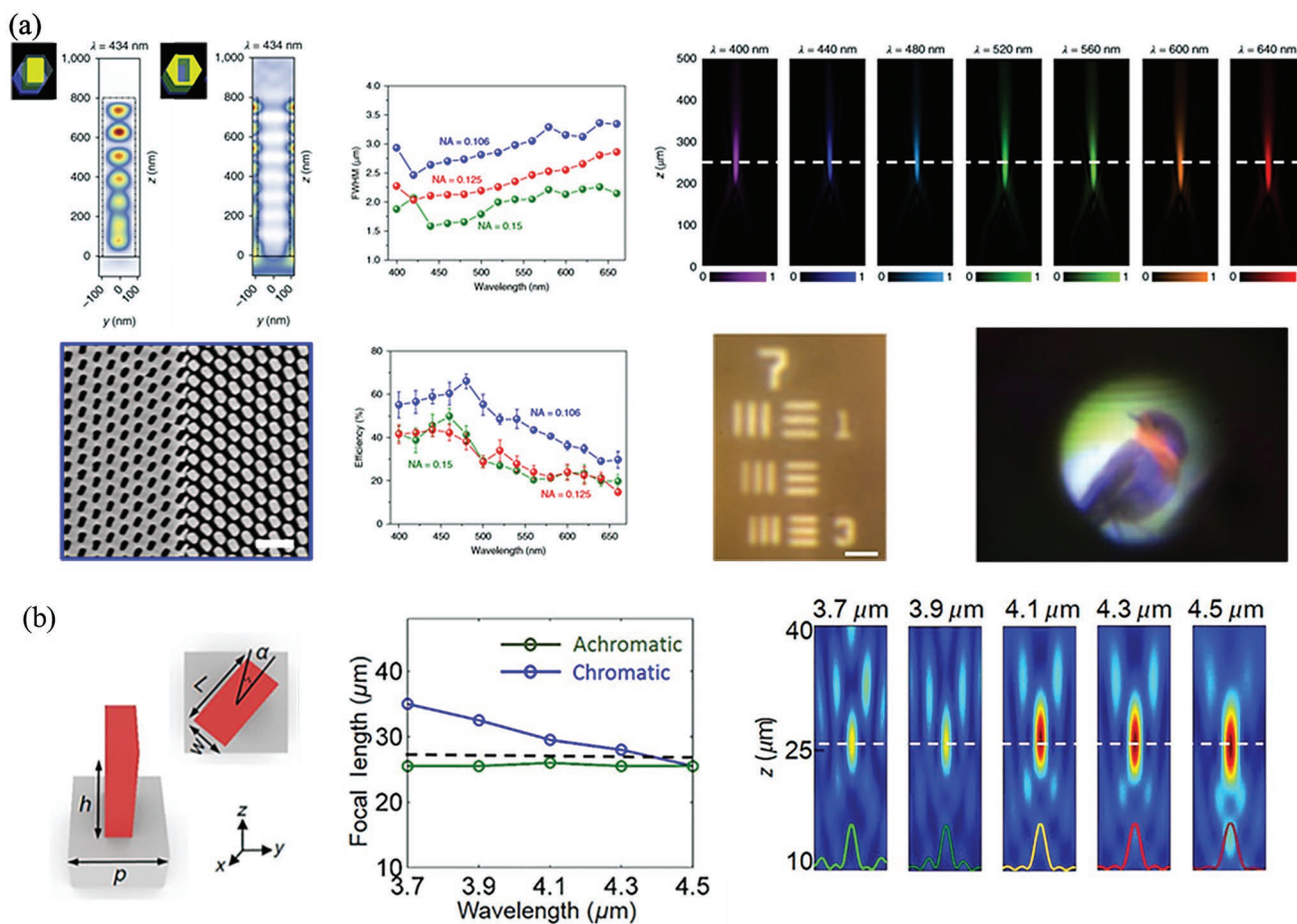
Figure 7. a) Metalens made of GaN nanopillars and nanoholes to demonstrate a constant focal length from 400 to 660 nm. b) Metalens made of Si nanobricks to realize an unchanged focal length from 3.7 to 4.5 μm. a) Reproduced with permission.[97] Copyright 2018, Springer Nature. b) Reproduced with permission.[98] Copyright 2019, American Physical Society.

essentially controlled by the effective index related to duty cycle. With high average efficiency of 40% over the whole visible spectrum and extraordinary minimum resolution of ≈2.19 μm the metalens with NA = 0.106 is successfully used into full-color imaging even video, shown as **Figure 7**a. With the same design mechanism, an achromatic metalens working over a broadband in the infrared region from 3.7 to 4.5 μm for circularly polarized incidences was proposed in simulation (see in Figure 7b).[98]

In a follow-up work, Lin et al. constructed an metalens array of 60 × 60 achromatic metalenses to demonstrate a full-color light-field camera with a diffraction-limited resolution of 1.95 μm.[99] It is possible to make a larger optical imaging system with the design of an achromatic metalens array and the SEM of the metalens array has been shown in **Figure 8**b. Based on a compact planar achromatic metalens array, the light field camera captures light field images for broadband focusing with chromatic aberration or spherical aberration. Each metalens captures a portion of the light field image. By full capture of 4D optical information, the method of digital image processing has been developed. By using computer image processing for refocusing light-field image, one can finally achieve rendered all-in-focus images (Figure 8c), rendered images focusing on different focusing length (Figure 8d), and estimated depth map

corresponding to image (Figure 8e). The realization of full-color, achromatic light-field camera open up new possibilities to the development of multifocusing microscopy, high-dimension quantum technology, hyperspectral microscopy, robotic microvision, unoccupied vehicle sensing, virtual and augmented reality, drones and miniature personal security systems.

In addition, Capasso and his collaborators utilized TiO$_2$ nanofins in close proximity as coupled waveguides combining with geometric phase to realize a transmissive broadband achromatic metalens in visible with a NA of 0.2.[100] In this work, the phase in Equation (1) can be expanded as a Taylor series near a design frequency ω_d as

$$\varphi(R,\omega) = \varphi(R,\omega_d) + \frac{\partial \varphi(R,\omega)}{\partial \omega}\bigg|_{\omega=\omega_d}(\omega-\omega_d) + \frac{\partial^2 \varphi(R,\omega)}{2\partial\omega^2}\bigg|_{\omega=\omega_d}(\omega-\omega_d)^2$$

(3)

the three terms represent the required relative phase, group delay and group delay dispersion, respectively. By judicious design of nanofins to satisfy phase, group even group delay dispersion, the broadband achromatic metalens is demonstrated from 470 to 670 nm with efficiency of about 20% at 500 nm. This metalens still shows a little chromatic aberration shown in
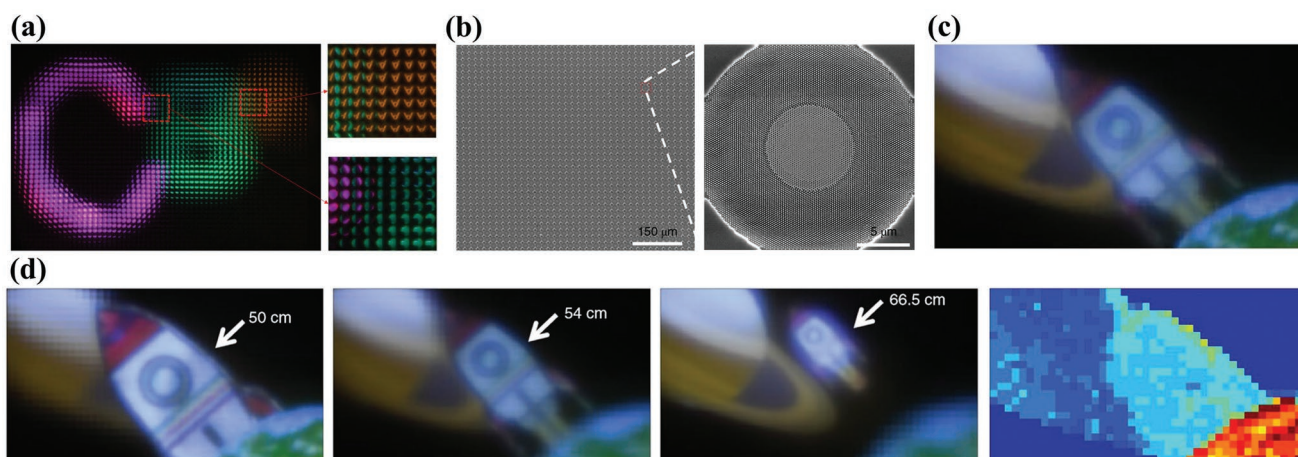
Figure 8. Full-color light-field imaging captured by GaN-based achromatic metalens array. a–d) Reproduced with permission.[99] Copyright 2019, Springer Nature.

the images under an illumination bandwidth of 200 nm centered at 570 nm (see in **Figure 9**). Though this design needs further optimization, the metalens achieves diffraction-limited achromatic focusing over almost the whole visible spectrum, a feat that traditionally requires the stacking of many refractive lenses with different glass materials and shapes. The realization of broadband achromatic and dispersion-tailored metalenses in visible has great significance in integrated imaging system, such as mobile lens, endoscopy, and virtual and augmented reality.

In previous works on broadband achromatic metalenses, limited by design principle almost all the metalenses only worked in circularly polarized illumination. However, polarization-insensitive metasurfaces are more desirable for practical applications. Recently Shrestha et al. demonstrated a polarization-independent broadband achromatic metalens in transmission version from 1200 to 1650 nm in the near infrared, which is complementary metal oxide semiconductor (CMOS)-compatible.[101] They created libraries of meta-units building blocks of metasurfaces-with complex cross-sectional geometries which can provide diverse phase dispersions for any arbitrary

polarized incident light while phase is a function of wavelength. By choosing nanostructures with proper geometric shape and parameter satisfying the phase and phase dispersion for the chosen bandwidth, a near-constant focal length over continuous 1200 to 1650 nm and focusing efficiencies up to 50% are realized through the polarization-independent achromatic metalens, shown as **Figure 10**a. These unprecedented properties represent a significant progress compared to the latest technology and an important step toward practical applications of metalenses, especially in shrinking imaging systems. But it cannot be ignored that a degree of freedom in the design space is lost due to the usage of symmetric constituent nanostructures for polarization-independence, which greatly restricts the ability to tailor phase of the metasurface devices.

Utilizing anisotropic TiO_2 nanostructures, which is different from the solution associated with spatial multiplexing and symmetry, Capasso and his collaborators demonstrated a broadband achromatic polarization-insensitive metalens with a NA of 0.2 over the visible range from 460 to 700 nm while maintaining diffraction-limited performance.[102] The design principle still
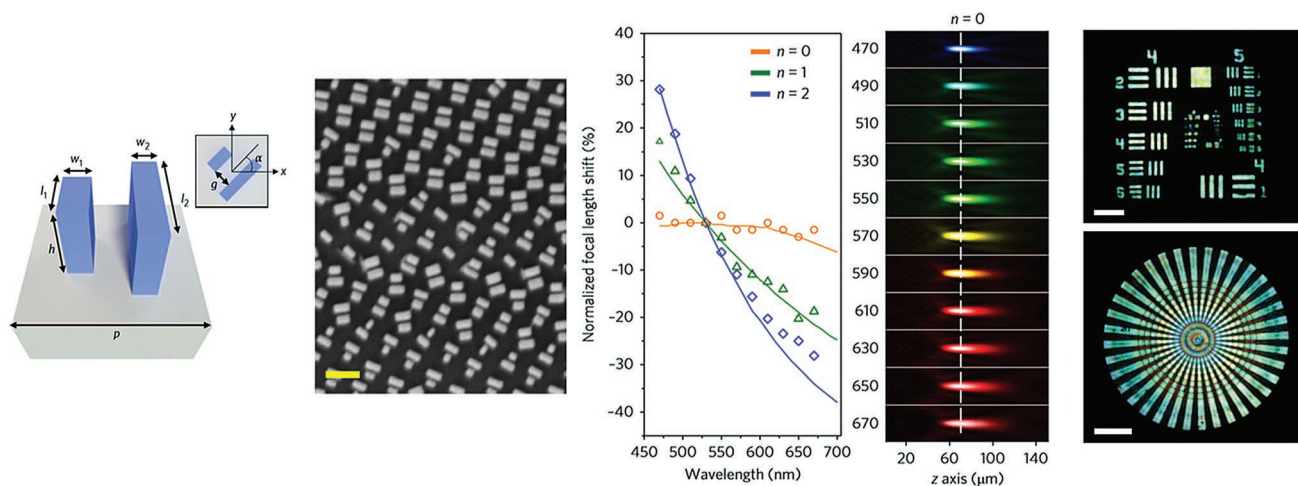

Figure 9. Metalens made of coupled TiO_2 nanofits to achieve achromatic imaging from 470 to 670 nm. Reproduced with permission.[100] Copyright 2018, Springer Nature.

1904935 (12 of 20)

ADVANCED
SCIENCE NEWS
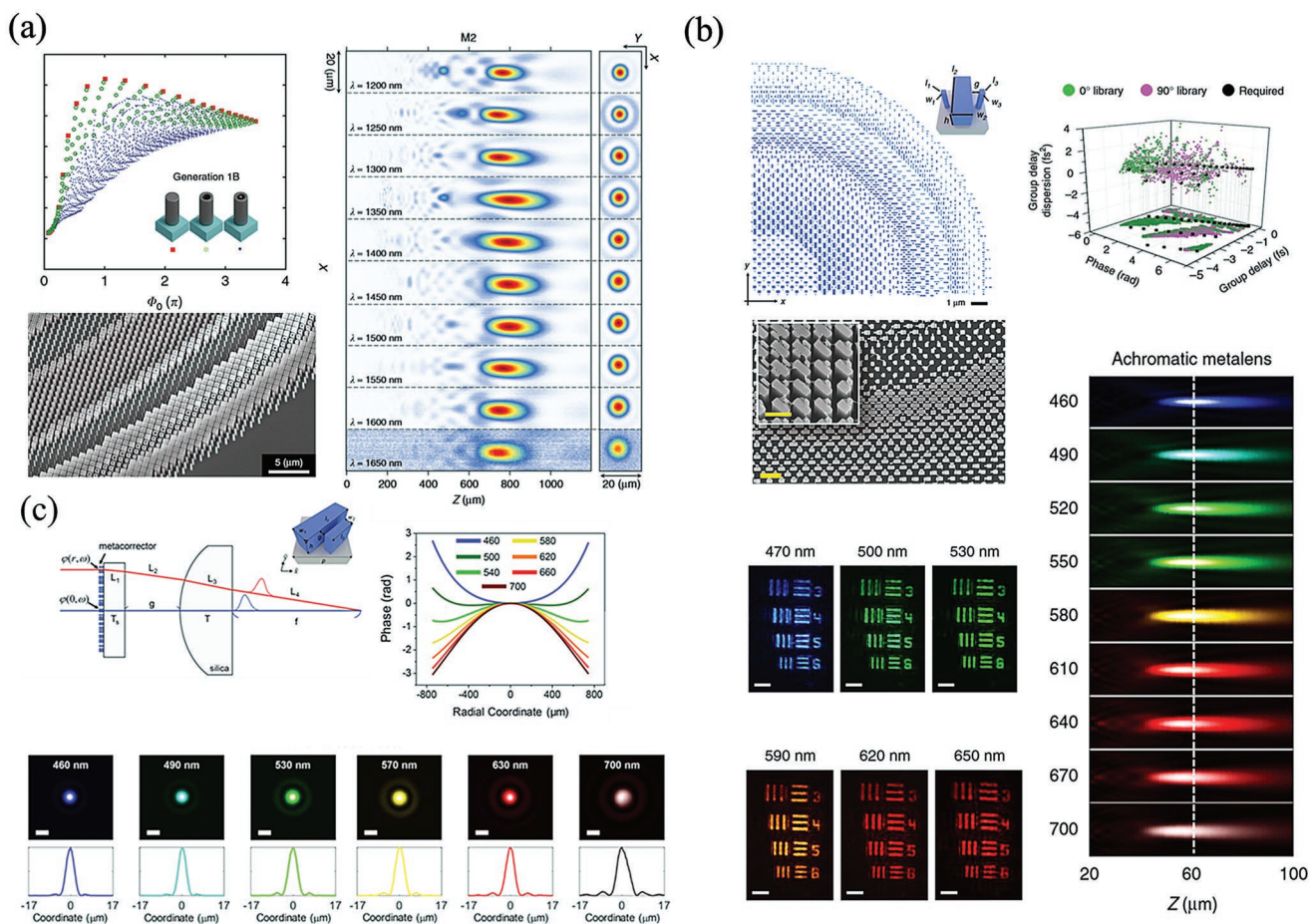www.advancedsciencenews.com

ADVANCED
MATERIALS
www.advmat.de

Figure 10. a) Broadband achromatic metalenses with any arbitrary polarization state from 1200–1650 nm. b) Broadband achromatic polarization-insensitive metalens over the visible range from 460 to 700 nm. c) Broadband achromatic metasurface-refractive device by combining metasurfaces and traditional refractive optical components. a) Reproduced under the terms of the CC-BY Creative Commons Attribution 4.0 International License (http://creativecommons.org/licenses/by/4.0/).[101] Copyright 2018, The Authors, published by Springer Nature. b) Reproduced under the terms of the CC-BY Creative Commons Attribution 4.0 International License (http://creativecommons.org/licenses/by/4.0/).[102] Copyright 2019, The Authors, published by Springer Nature. c) Reproduced with permission.[103] Copyright 2018, American Chemical Society.

involves geometric phase, but the polarization-dependence is avoided by limiting the rotation angle of each anisotropic element to either 0° or 90°, meanwhile the freedom to impart an additional π phase shift is offered. Each element consists of multiple nanofins, which have more geometric parameters so that additional degrees of freedom are provided to better engineer the dispersion. By controlling the length, width and gap of nanofins, they implemented the phase and its two higher order derivatives (group delay and group delay dispersion) with respect to frequency in Equation (3) and realized the broadband achromatic polarization-insensitive metalens in both simulations and experiments. The selection and design of nanofins, SEM image of the metalens and its focusing effect and imaging at different wavelengths are respectively exhibited in Figure 10b. This design approach of polarization-independence provides metasurface devices with more applications in imaging, augmented reality and other integrated optics. According to the works mentioned above, single-layer broadband achromatic metasurface lenses have already been demonstrated. However, due to the large required group delays, diameters of broadband

achromatic metalens limits on the order of 100 μm. Chen et al. designed a broadband achromatic metasurface-refractive device in visible by combining a tunable phase and artificial dispersion to correct spherical and chromatic aberrations in a large spherical plano-convex lens (see in Figure 10c).[103] The united metasurfaces and traditional lenses overcome the challenging of achieving the required group delay range across the metalens. The great performance has further validated by designing a metacorrector, which greatly increases the bandwidth of a state-of-the-art immersion objective. The combination of metasurfaces and traditional refractive optical components brings tremendous progress in simplification and miniaturization of optical devices.

6. Super Dispersion and Other Chromatic Applications

Contrary to achromatic metalenses able to focus light with different wavelengths into the same spot spatially, metasurfaces with super dispersion are designed to increase chromatic aberration and separate the different wavelength of light more
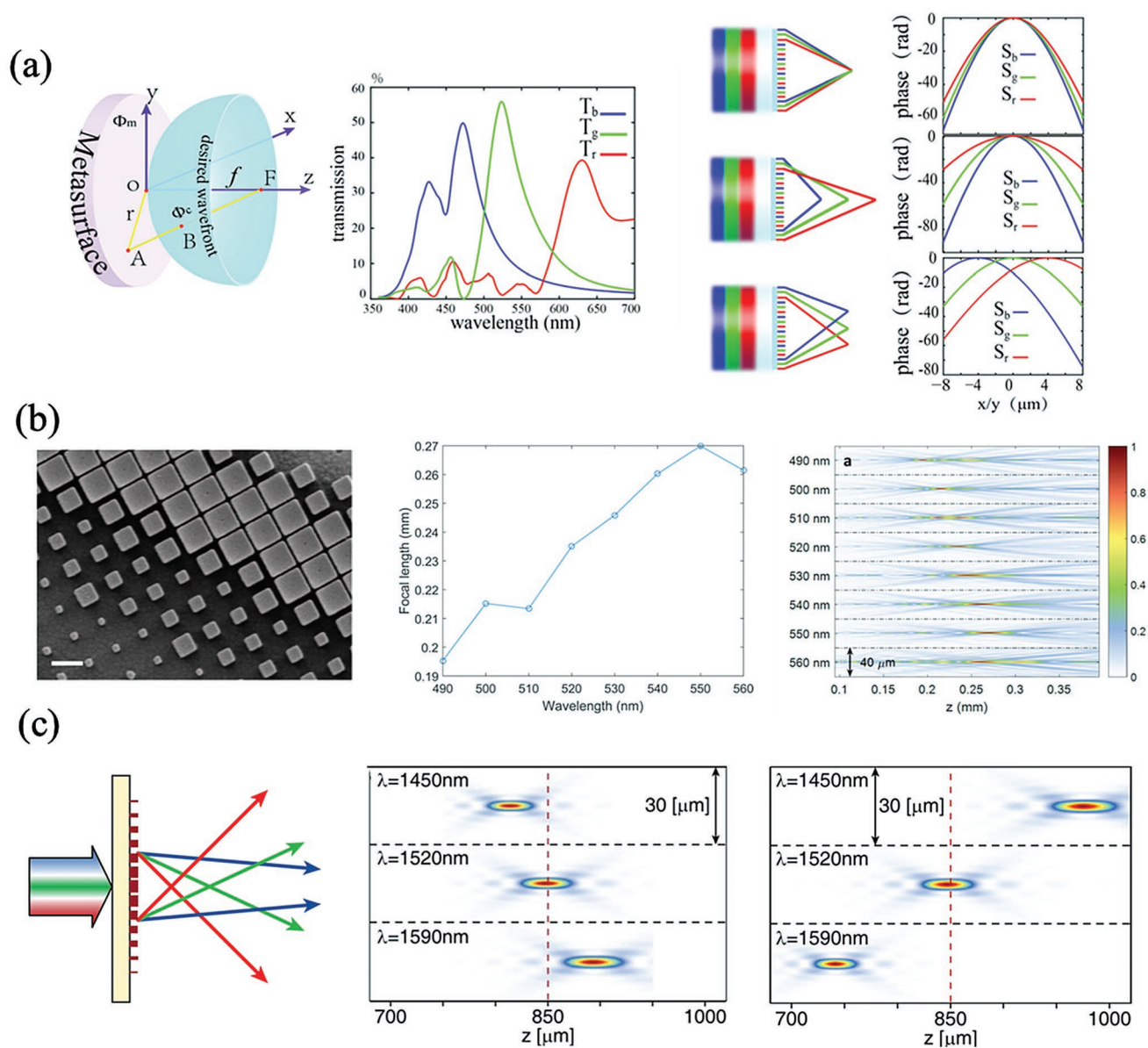
Figure 11. a) Multiplexing dielectric metalenses realize arbitrary dispersion. b) Metalenses with reverse chromatic dispersion design. c) Hyperpositive and hypernegative dispersion metalenses based on square nanopillars. a) Reproduced with permission.[85] Copyright 2017, Optical Society of America. b) Reproduced with permission.[94] Copyright 2017, American Chemical Society. c) Reproduced with permission.[95] Copyright 2017, Optical Society of America.

widely in space. Several design principles of achromatic metalenses mentioned above can be also used for super chromatic dispersion metalenses. Li et al. showed the a series of spatial multiplexing dielectric metalenses able to realize arbitrary dispersion for three visible frequencies in simulation (**Figure 11**a).[85] A metalens with reverse chromatic dispersion with focal length increasing as the wavelength increases was designed over 60 nm bandwidth in visible by Capasso and his collaborators (Figure 11b).[94] Faraon and co-workers also demonstrated the hyper-positive and hyper-negative dispersion metalenses over the operation bandwidth of 1450 to 1590 nm in near infrared (Figure 11c).[95]

Obviously in many optical systems especially colorful imaging devices, the chromatic aberration of metalenses have a negative

impact on their performance, but in some applications carefully designed super dispersion can be utilized to optimize or implement optical devices with specific functions, for example spectrometer. In the traditional spectrometer, the distance between the grating and detector needs to be very large in order to improve the spectral resolution, which makes high resolution spectrometer particularly cumbersome. Off-axis metalenses that combines focus and disperse light at different wavelengths with very high spectral resolution were demonstrated by Capasso and his collaborators.[104] Silicon nanofins were used as meta-units and the phase requirement was implemented based on the geometric phase via rotated nanofins. With carefully tailoring the chromatic dispersion of the metalens, lights can be focused in a focal line parallel to the metalens with focusing angles as large
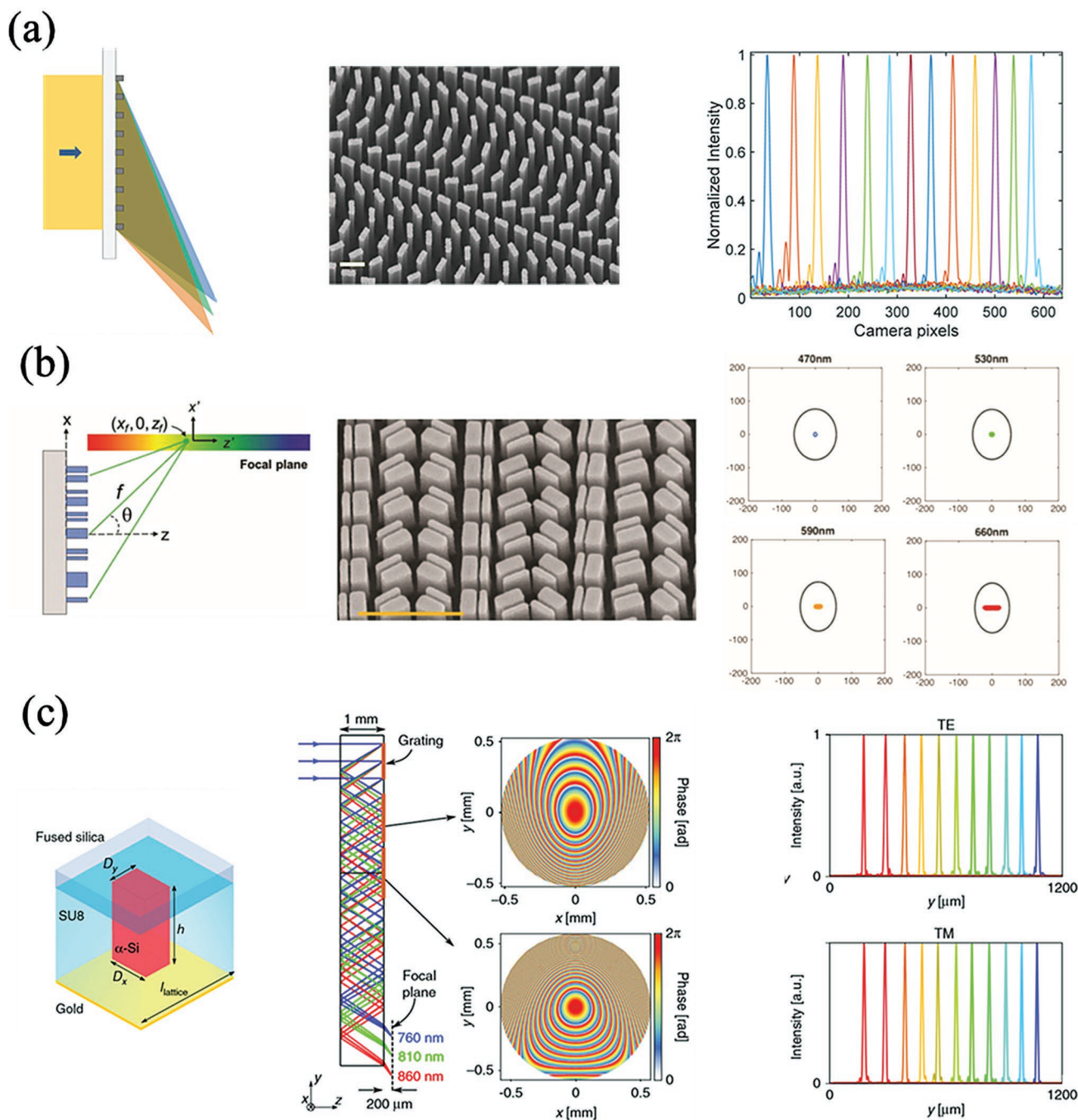
ADVANCED
SCIENCE NEWS
www.advancedsciencenews.com

ADVANCED
MATERIALS
www.advmat.de

Figure 12. a) High spectral resolution realized by off-axis metalenses. b) A spectrometer maintaining its focal spot profile along a plane across visible range. c) A spectrometer consisting of three reflective silicon metasurfaces. a) Reproduced with permission.[104] Copyright 2016, American Chemical Society. b) Reproduced with permission.[105] Copyright 2018, Wiley-VCH. c) Reproduced under the terms of the CC-BY Creative Commons Attribution 4.0 International License (http://creativecommons.org/licenses/by/4.0/).[106] Copyright 2018, The Authors, published by Springer Nature.

as 80°. The focused point shifts along the focal line at different wavelengths, which is utilized to resolve the incident wavelengths with high precision, and the spectral resolution increases with focusing angle. Because of the large angle of focus, these metalenses have super dispersion of 0.27 nm mrad^{-1}, which enables them to distinguish the wavelength difference of less than 200 pm in the telecom area (**Figure 12**a). In the range

of 1100 to 1600 nm the operation efficiency can reach up to 90%. In addition, a higher spectral resolution in a wider wavelength range can be maintained by stitching several metalenses together. With the verification of hyperspectral resolution, off-axis with super dispersion have good feasibility for compact and portable/wearable optical applications. Later a compact aberration-corrected spectrometer in visible region was demonstrated

by the same research group, which consists of polarization-independent TiO_2 nanofins.[105] The off-axis metalens used in this spectrometer maintains its focal spot profile along a plane and undergo minimal focal spot broadening for almost 200 nm across the visible range (Figure 12b). With a working distance of only 4 cm, the miniature aberration-corrected spectrometer has high spectral resolutions of 0.96, 1.01, 1.06, and 1.14 nm at 488, 532, 632, and 660 nm incident wavelengths, respectively. For further integration, with the concept of folded metasurface optics, Faraon and co-workers demonstrated a compact spectrometer with a volume of only 7 mm³.[106] This spectrometer consists of three reflective silicon metasurfaces on one side of a 1 mm thick glass slab backed by gold mirrors. Through several accumulations of tailored chromatic dispersion and light propagation, the spectrometer has a high resolution of ≈1.2 nm across a spectral range from 760 to 860 nm (Figure 12c).

As a planar optical device, metasurfaces have the advantages of ultra-thin, lightweight, and ultra-compact. With high degree of freedom metasurfaces can realize various functions which are impossible in traditional devices. Besides color imaging based on achromatism, spectroscopy based on super dispersion, there are many other applications of controlling the

chromatic dispersion with metasurfaces, including, nano-optic endoscope, full-color routing, and multiwavelength holograms, these we will discuss next.

Recently Pahlevaninezhad et al. have considered near diffraction-limited imaging through an endoscopic optical coherence tomography catheter, which is integrated with a metalens controlling the phase and negating nonchromatic aberrations.[107] The metalens is composed of amorphous silicon nanopillar with a fixed height and varying diameters of circular cross-section to locally impart the phase requirement. The azimuthal symmetry of these nanopillars results in polarization-insensitive metalens with very small incident angles. It is worth noting that in the context of spectral interferometry the engineered chromatic dispersion of the metalens is used to maintain high resolution imaging beyond the input field Rayleigh range, thus alleviating the trade-off between transverse resolution and depth of focus. The combination of the superior resolution and higher imaging depth of focus increases the clinical utility of endoscopic optical imaging. The endoscopic imaging is demonstrated in living resected organic specimens (**Figure 13**a).

Chen et al. demonstrated a highly efficient dielectric metalens in a complementary metal-oxide-semiconductor sensor
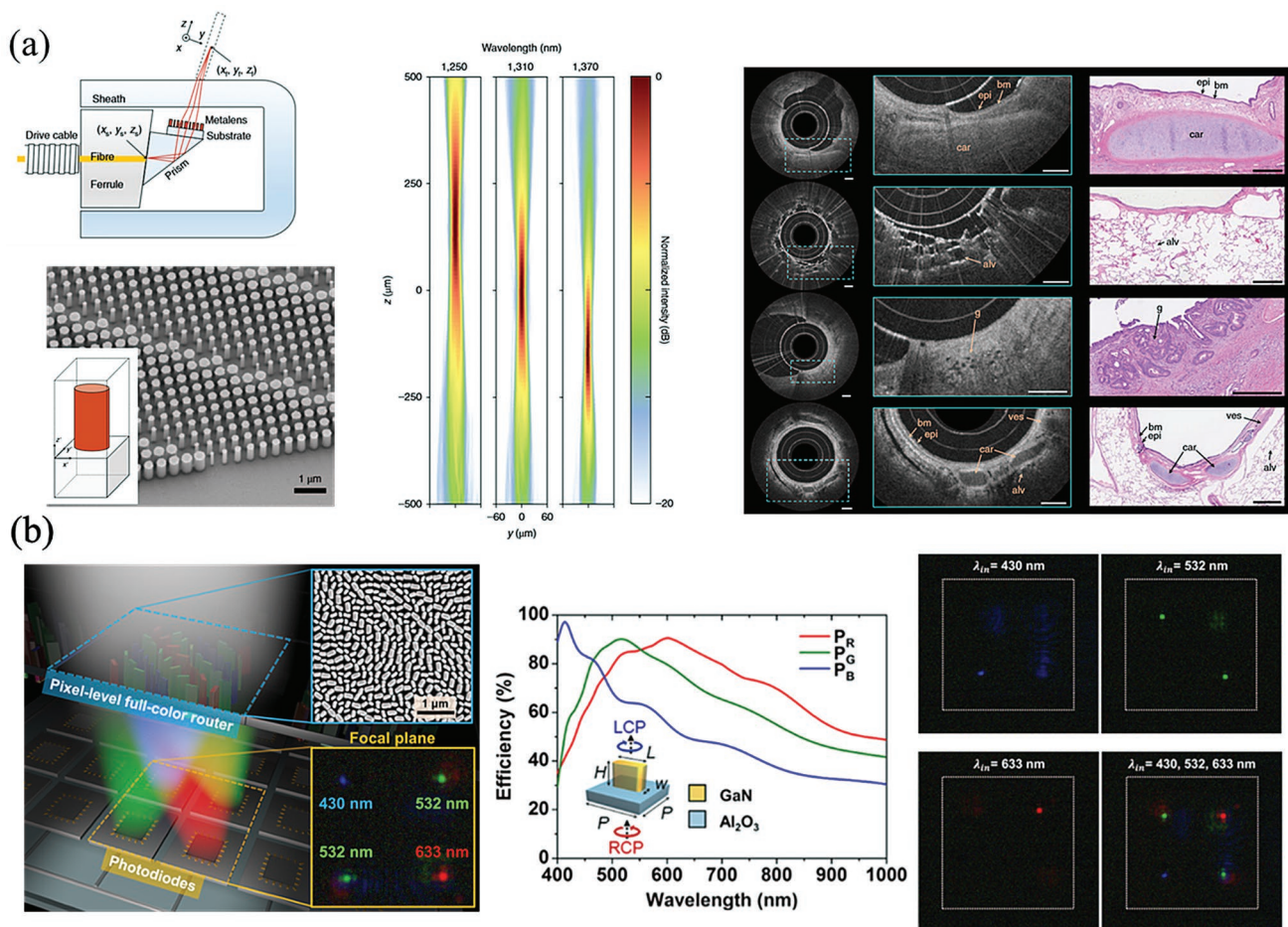

Figure 13. a) Metalens with engineered chromatic dispersion for high resolution optical coherence tomography images. b) Multiplex metalens design for color routing in visible image. a) Reproduced with permission.[107] Copyright 2018, Springer Nature. b) Reproduced with permission.[108] Copyright 2017, American Chemical Society.

**ADVANCED
SCIENCE NEWS**

www.advancedsciencenews.com

**ADVANCED
MATERIALS**

www.advmat.de

whose focal spot can be passively controlled to arbitrary location in free space at visible light (Figure 13b).[108] By integrating different GaN-based dielectric metalenses directing three colors onto the correspondingly desired spatial positions into one, the multiplex color router are able to focus three individual primary colors (RGB) to any spatial positions. In experiment, the focusing efficiencies of multiplex color router are up to 87%, 91.6%, and 50.6% for blue, green and red lights, respectively. Different from the super-dispersive off-axis metalenses, the multiplex color router offers more degrees of freedom to focus lights of different wavelengths to any position independently. Due to its low-cost, semiconductor fabrication compatibility, and high efficiency, this approach is also applicable to a wide

range of integrated optical devices, such as high-resolution lithography, compact imaging sensors, optical spectroscopy, and optical communications.

Luo and co-workers experimentally demonstrated a full-color meta-hologram in the 3D space.[109] On the basis of the off-axis illumination method, a new approach to overcome the cross-talk among different colors was proposed and finally a single type of plasmonic pixel realized multicolor meta-holography. The building block to construct the meta-hologram is a set of nanoslit antennas, which is efficient for a broadband wavelength in the visible range from 380 to 780 nm based on geometric phase to modulate the phase. This achromatic feature is the key feature to separate and position the image patterns
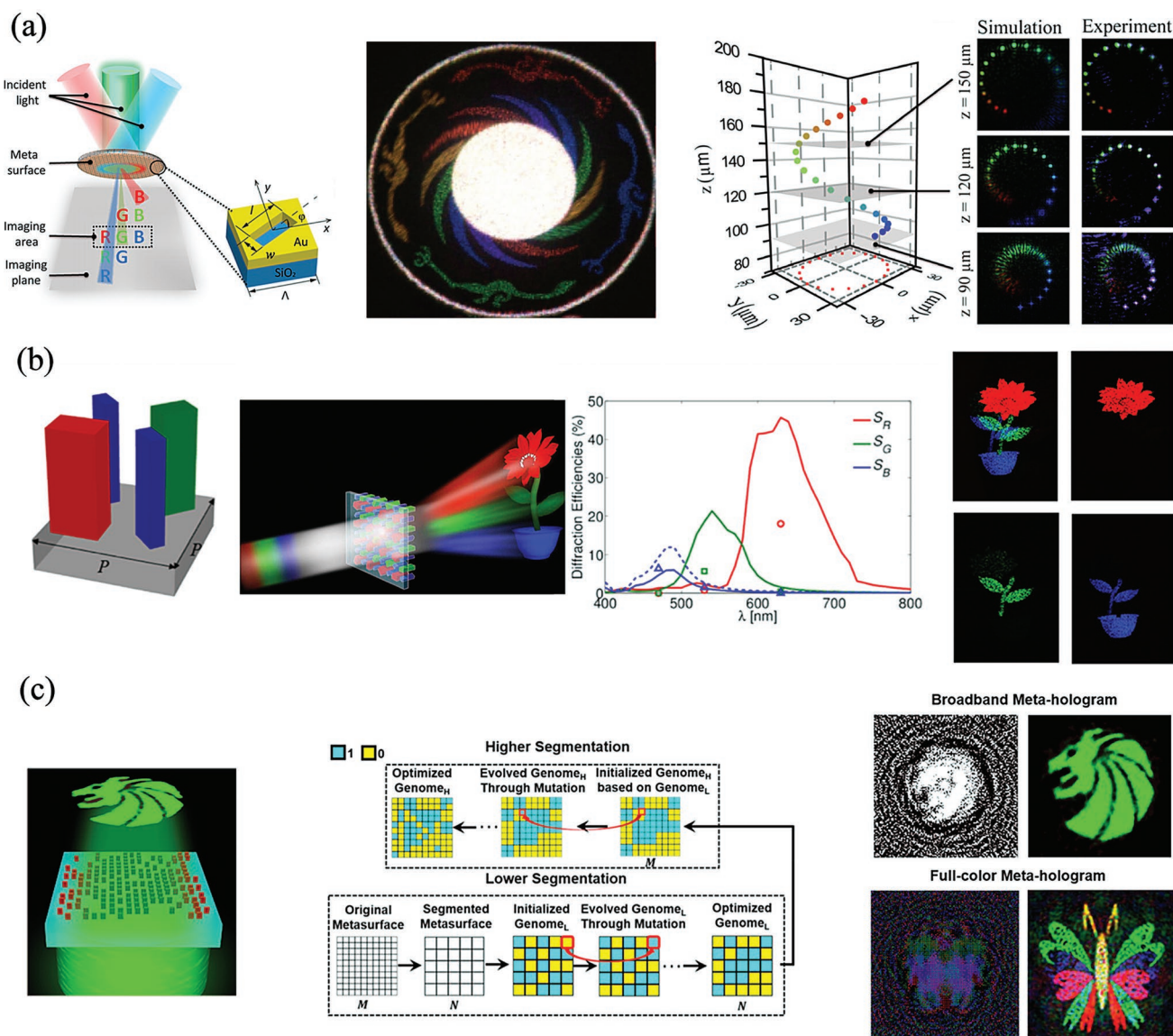

Figure 14. a) Multicolor 3D meta-hologram display by broadband plasmonic modulation. b) Dielectric metasurfaces for multiwavelength achromatic and highly dispersive holograms. c) Broadband and full-color hologram by segmented hierarchical evolutionary algorithm. a) Reproduced with permission.[109] Copyright 2016, The Authors, published by American Association for the Advancement of Science (AAAS). Reprinted/modified from ref. [109]. © The Authors, some rights reserved; exclusive licensee American Association for the Advancement of Science. Distributed under a Creative Commons Attribution NonCommercial License 4.0 (CC BY-NC) http://creativecommons.org/licenses/by-nc/4.0/. b) Reproduced with permission.[110] Copyright 2016, American Chemical Society. c) Reproduced with permission.[111] Copyright 2019, American Chemical Society.

**ADVANCED
SCIENCE NEWS**

www.advancedsciencenews.com

**ADVANCED
MATERIALS**

www.advmat.de

corresponding to different colors at different spatial locations, thus the cross-talk among colors is eliminated. The schematic of the methodology, multi-image hologram, seven color meta-hologram and the stars map 3D imaging are shown in **Figure 14**a, respectively. This approach not only overcomes the fundamental cross-talk limitation and improves the signal to noise ratio (SNR) in this field, but also provides new opportunities to design functional devices that have never been realized before. Wang et al. showed that multiplexed dielectric metasurfaces also can be used to demonstrate multiwavelength achromatic and highly dispersive holograms.[110] The metasurface is composed of silicon nanoblocks with three sizes multiplexed with subwavelength spacing to manipulate the phases of red, green, and blue color. The strong confinement of light in these nanoblocks basically avoids their interaction in each unit so that the phase of each color can be controlled by geometric phase without any cross-talk. The experimental results of achromatic color hologram and highly dispersive color holograms are shown in Figure 14b. This technique has the potential for multiwavelength applications that requires the independent wavefront control among different wavelengths. In addition, experimental demonstration of the full-color meta-holograms have been also realized by a segmented hierarchical evolutionary algorithm, which is able to solve large-pixelated, complex inverse meta-optics design, shown as Figure 14c.[111]

7. Conclusion and Discussion

In summary, we have reviewed the recent development of chromatic dispersion manipulation based on metalenses. Various approaches for cancelling the chromatic aberration in metalenses have been proposed to realize multiwavelength achromatism, narrow band achromatism and broadband achromatism in different wavelength region. These achievements are of great importance in metalens design with high requirement in bandwidth. On the other hand, the chromatic dispersion can also be utilized to manage special functionalities, such as spectrometer, OCT, multicolor hologram, etc. In the past few years, many excellent works have been carried out and fruitful achievements have been obtained based on the chromatic dispersion. We believe that there will be more and more researches emerged with the further using of chromatic dispersion of metalens. For example, the spectral imaging camera is usually composed of several optical elements, such as mask, grating (or prism), lens, etc. The dispersion engineered metalenses can fulfill the function of these elements at a single piece, which can greatly miniaturize of size of the system. In other cases, such as full-color AR and VR system, biological examination and detection, etc., chromatic dispersion manipulation of metalenses is also quite desired to promote metalenses into real applications. Beyond that, as a flat lens with precise control ability, metalens also have broad compact application prospects in the combination of traditional optical lenses in the foreseeable future. Meta-design can be applied to correct residual aberrations in traditional lenses, compensate for chromatic aberrations, and achieve more perfect optical imaging effect. Based on this, we believe that metalenses will promote the development of integrated optical devices with special needs, such as space and ocean exploration, mobile phone lens and wearable devices.

[1] Y. W. Huang, W. T. Chen, W. Y. Tsai, P. C. Wu, C. M. Wang, G. Sun, D. P. Tsai, *Nano Lett.* **2015**, *15*, 3122.

[2] M. Khorasaninejad, W. T. Chen, A. Y. Zhu, J. Oh, R. C. Devlin, D. Rousso, F. Capasso, *Nano Lett.* **2016**, *16*, 4595.

[3] M. Pu, X. Li, X. Ma, Y. Wang, Z. Zhao, C. Wang, C. Hu, P. Gao, C. Huang, H. Ren, X. Li, F. Qin, J. Yang, M. Gu, M. Hong, X. Luo, *Sci. Adv.* **2015**, *1*, e1500396.

[4] W. T. Chen, P. Török, M. R. Foreman, C. Y. Liao, W.-Y. Tsai, P. R. Wu, D. P. Tsai, *Nanotechnology* **2016**, *27*, 224002.

[5] M. Khorasaninejad, W. T. Chen, R. C. Devlin, J. Oh, A. Y. Zhu, F. Capasso, *Science* **2016**, *352*, 1190.

[6] X. Chen, L. Huang, H. Mühlenbernd, G. Li, B. Bai, Q. Tan, G. Jin, C. W. Qiu, S. Zhang, T. Zentgraf, *Nat. Commun.* **2012**, *3*, 1198.

[7] D. Wen, F. Yue, G. Li, G. Zheng, K. Chan, S. Chen, M. Chen, K. F. Li, P. W. H. Wong, K. W. Cheah, E. Yue Bun Pun, S. Zhang, X. Chen, *Nat. Commun.* **2015**, *6*, 8241.

[8] L. Wang, S. Kruk, H. Tang, T. Li, I. Kravchenko, D. N. Neshev, Y. S. Kivshar, *Optica* **2016**, *3*, 1504.

[9] P. Cheben, R. Halir, J. H. Schmid, H. A. Atwater, D. R. Smith, *Nature* **2018**, *560*, 565.

[10] C. C. Chen, A. Ishikawa, Y. H. Tang, M. H. Shiao, D. P. Tsai, T. Tanaka, *Adv. Opt. Mater.* **2015**, *3*, 44.

[11] A. Davoyan, H. Atwater, *Optica* **2018**, *5*, 608.

[12] P. N. Dyachenko, S. Molesky, A. Y. Petrov, M. Stormer, T. Krekeler, S. Lang, M. Ritter, Z. Jacob, M. Eich, *Nat. Commun.* **2016**, *7*, 11809.

[13] Y. W. Huang, H. W. Lee, R. Sokhoyan, R. A. Pala, K. Thyagarajan, S. Han, D. P. Tsai, H. A. Atwater, *Nano Lett.* **2016**, *16*, 5319.

[14] S. Jahani, Z. Jacob, *Nat. Nanotechnol.* **2016**, *11*, 23.

[15] S. Jahani, S. Kim, J. Atkinson, J. C. Wirth, F. Kalhor, A. A. Noman, W. D. Newman, P. Shekhar, K. Han, V. Van, R. G. DeCorby, L. Chrostowski, M. Qi, Z. Jacob, *Nat. Commun.* **2018**, *9*, 1893.

[16] P. V. Kapitanova, P. Ginzburg, F. J. Rodriguez-Fortuno, D. S. Filonov, P. M. Voroshilov, P. A. Belov, A. N. Poddubny, Y. S. Kivshar, G. A. Wurtz, A. V. Zayats, *Nat. Commun.* **2014**, *5*, 3226.

[17] H. N. Krishnamoorthy, Z. Jacob, E. Narimanov, I. Kretzschmar, V. M. Menon, *Science* **2012**, *336*, 205.

[18] A. I. Kuznetsov, A. E. Miroshnichenko, M. L. Brongersma, Y. S. Kivshar, B. Lukyanchuk, *Science* **2016**, *354*, aag2472.

[19] Z. Liu, D. Zhu, S. P. Rodrigues, K. T. Lee, W. Cai, *Nano Lett.* **2018**, *18*, 6570.

[20] R. Mudachathi, T. Tanaka, *Sci. Rep.* **2017**, *7*, 1199.

[21] L. H. Nicholls, F. J. Rodríguez-Fortuño, M. E. Nasir, R. M. Córdova-Castro, N. Olivier, G. A. Wurtz, A. V. Zayats, *Nat. Photonics* **2017**, *11*, 628.

[22] Y. Park, C. Depeursinge, G. Popescu, *Nat. Photonics* **2018**, *12*, 578.

[23] J. Rho, Z. Ye, Y. Xiong, X. Yin, Z. Liu, H. Choi, G. Bartal, X. Zhang, *Nat. Commun.* **2010**, *1*, 143.

[24] M. C. Sherrott, P. W. C. Hon, K. T. Fountaine, J. C. Garcia, S. M. Ponti, V. W. Brar, L. A. Sweatlock, H. A. Atwater, *Nano Lett.* **2017**, *17*, 3027.

[25] K. Thyagarajan, R. Sokhoyan, L. Zornberg, H. A. Atwater, *Adv. Mater.* **2017**, *29*, 1701044.

[26] C. Wang, M. Zhang, X. Chen, M. Bertrand, A. Shams-Ansari, S. Chandrasekhar, P. Winzer, M. Loncar, *Nature* **2018**, *562*, 101.

[27] K. Wu, P. Coquet, Q. J. Wang, P. Genevet, *Nat. Commun.* **2018**, *9*, 3494.

[28] X. Yin, Z. Ye, J. Rho, Y. Wang, X. Zhang, *Science* **2013**, *339*, 1405.

[29] L. Zhang, X. Q. Chen, S. Liu, Q. Zhang, J. Zhao, J. Y. Dai, G. D. Bai, X. Wan, Q. Cheng, G. Castaldi, V. Galdi, T. J. Cui, *Nat. Commun.* **2018**, *9*, 4334.

[30] X. Chen, Y. Zhang, L. Huang, S. Zhang, *Adv. Opt. Mater.* **2014**, *2*, 978.

[31] S. Sun, K. Y. Yang, C. M. Wang, T. K. Chen, C. Y. Liao, Q. He, S. Xiao, W. T. Kung, G. Y. Guo, L. Zhou, D. P. Tsai, *Nano Lett.* **2012**, *12*, 6223.

[32] B. Walther, C. Helgert, C. Rockstuhl, F. Setzpfandt, F. Eilenberger, E.-B. Kley, F. Lederer, A. Tünnermann, T. Pertsch, *Adv. Mater.* **2012**, *24*, 6251.

[33] J. Lin, J. P. B. Mueller, Q. Wang, G. Yuan, N. Antoniou, X. C. Yuan, F. Capasso, *Science* **2013**, *340*, 331.

[34] L. Li, T. Li, X. M. Tang, S. M. Wang, Q. J. Wang, S. N. Zhu, *Light: Sci. Appl* **2015**, *4*, e330.

[35] P. C. Wu, W. Zhu, Z. X. Shen, P. H. J. Chong, W. Ser, D. P. Tsai, A.-Q. Liu, *Adv. Opt. Mater.* **2017**, *5*, 1600938.

[36] K. Huang, Z. Dong, S. Mei, L. Zhang, Y. Liu, H. Liu, H. Zhu, J. Teng, B. Luk'yanchuk, J. K. W. Yang, C. W. Qiu, *Laser Photonics Rev.* **2016**, *10*, 500.

[37] G. Zheng, H. Muhlenbernd, M. Kenney, G. Li, T. Zentgraf, S. Zhang, *Nat. Nanotechnol.* **2015**, *10*, 308.

[38] X. Ni, A. V. Kildishev, V. M. Shalaev, *Nat. Commun.* **2013**, *4*, 2807.

[39] W. T. Chen, K. Y. Yang, C. M. Wang, Y. W. Huang, G. Sun, I. D. Chiang, W. L. Chun, W. L. Hsu, H. T. Lin, S. Sun, L. Zhou, A. Q. Liu, D. P. Tsai, *Nano Lett.* **2014**, *14*, 225.

[40] M. Khorasaninejad, A. Ambrosio, P. Kanhaiya, F. Capasso, *Sci. Adv.* **2016**, *2*, e1501258.

[41] K. C. Shen, C. T. Ku, C. Hsieh, H. C. Kuo, Y. J. Cheng, D. P. Tsai, *Adv. Mater.* **2018**, *30*, 1706918.

[42] J. S. Totero Gongora, A. E. Miroshnichenko, Y. S. Kivshar, A. Fratalocchi, *Nat. Commun.* **2017**, *8*, 15535.

[43] Q. Zhang, G. Li, X. Liu, F. Qian, Y. Li, T. C. Sum, C. M. Lieber, Q. Xiong, *Nat. Commun.* **2014**, *5*, 4953.

[44] W. Zhou, M. Dridi, J. Y. Suh, C. H. Kim, D. T. Co, M. R. Wasielewski, G. C. Schatz, T. W. Odom, *Nat. Nanotechnol.* **2013**, *8*, 506.

[45] N. I. Zheludev, S. L. Prosvirnin, N. Papasimakis, V. A. Fedotov, *Nat. Photonics* **2008**, *2*, 351.

[46] G. Shangjr, S. Chih-Kang, *Rep. Prog. Phys.* **2016**, *79*, 086501.

[47] N. Yu, P. Genevet, M. A. Kats, F. Aieta, J. P. Tetienne, F. Capasso, Z. Gaburro, *Science* **2011**, *334*, 333.

[48] X. Ni, Z. J. Wong, M. Mrejen, Y. Wang, X. Zhang, *Science* **2015**, *349*, 1310.

[49] L. Huang, H. Mühlenbernd, X. Li, X. Song, B. Bai, Y. Wang, T. Zentgraf, *Adv. Mater.* **2015**, *27*, 6444.

[50] N. Dabidian, S. Dutta-Gupta, I. Kholmanov, K. Lai, F. Lu, J. Lee, M. Jin, S. Trendafilov, A. Khanikaev, B. Fallahazad, E. Tutuc, M. A. Belkin, G. Shvets, *Nano Lett.* **2016**, *16*, 3607.

[51] P. C. Wu, W.-Y. Tsai, W. T. Chen, Y.-W. Huang, T.-Y. Chen, J.-W. Chen, C. Y. Liao, C. H. Chu, G. Sun, D. P. Tsai, *Nano Lett.* **2017**, *17*, 445.

[52] T. Stav, A. Faerman, E. Maguid, D. Oren, V. Kleiner, E. Hasman, M. Segev, *Science* **2018**, *361*, 1101.

[53] G. Li, S. Zhang, T. Zentgraf, *Nat. Rev. Mater.* **2017**, *2*, 17010.

[54] M. Kauranen, A. V. Zayats, *Nat. Photonics* **2012**, *6*, 737.

[55] M. Celebrano, X. Wu, M. Baselli, S. Großmann, P. Biagioni, A. Locatelli, C. D. Angelis, G. Cerullo, R. Osellam, B. Hecht, L. Duò, F. Ciccacci, M. Finazzi, *Nat. Nanotechnol.* **2015**, *10*, 412.

[56] H. Aouani, M. Rahmani, M. Navarro-Cia, S. A. Maier, *Nat. Nanotechnol.* **2014**, *9*, 290.

[57] G. Vampa, B. G. Ghamsari, S. S. Mousavi, T. J. Hammond, A. Olivieri, L. Skrek, A. Y. Naumov, D. M. Villeneuve, A. Staudte, P. Berini, P. B. Corkum, *Nat. Phys.* **2017**, *13*, 659.

[58] D. A. Smirnova, A. B. Khanikaev, L. A. Smirnov, Y. S. Kivshar, *ACS Photonics* **2016**, *3*, 1468.

[59] M. Semmlinger, M. L. Tseng, J. Yang, M. Zhang, C. Zhang, W. Y. Tsai, D. P. Tsai, P. Nordlander, N. J. Halas, *Nano Lett.* **2018**, *18*, 5738.

[60] S. Liu, P. P. Vabishchevich, A. Vaskin, J. L. Reno, G. A. Keeler, M. B. Sinclair, I. Staude, I. Brener, *Nat. Commun.* **2018**, *9*, 2507.

[61] N. Segal, S. Keren-Zur, N. Hendler, T. Ellenbogen, *Nat. Photonics* **2015**, *9*, 180.

[62] E. Almeida, G. Shalem, Y. Prior, *Nat. Commun.* **2016**, *7*, 10367.

[63] X. Yang, C. Zhang, M. Wan, Z. Chen, Z. Wang, *Opt. Lett.* **2016**, *41*, 2938.

[64] G. Li, S. Chen, N. Pholchai, B. Reineke, P. W. H. Hong, E. Y. B. Pun, K. W. Cheah, T. Zentgraf, S. Zhang, *Nat. Mater.* **2015**, *14*, 607.

[65] X. Yang, W. Zang, M. Ma, P. Zhan, Z. Chen, Z. Wang, *Opt. Express* **2017**, *25*, 28363.

[66] E. Almeida, O. Bitton, Y. Prior, *Nat. Commun.* **2016**, *7*, 12533.

[67] W. Ye, F. Zeuner, X. Li, B. Reineke, S. He, C. W. Qiu, J. Liu, Y. Wang, S. Zhang, T. Zentgraf, *Nat. Commun.* **2016**, *7*, 11930.

[68] W. Zang, Z. Qin, X. Yang, Z. Chen, S. Wang, Z. Wang, *Adv. Opt. Mater.* **2019**, *7*, 1801747.

[69] S. Keren-Zur, O. Avayu, L. Michaeli, T. Ellenbogen, *ACS Photonics* **2016**, *3*, 117.

[70] R. Paniagua-Domínguez, Y. F. Yu, E. Khaidarov, S. Choi, V. Leong, R. M. Bakker, X. Liang, Y. H. Fu, V. Valuckas, L. A. Krivitsky, A. I. Kuznetsov, *Nano Lett.* **2018**, *18*, 2124.

[71] E. Arbabi, A. Arbabi, S. M. Kamali, Y. Horie, M. Faraji-Dana, A. Faraon, *Nat. Commun.* **2018**, *9*, 812.

[72] A. Arbabi, E. Arbabi, S. M. Kamali, Y. Horie, S. Han, A. Faraon, *Nat. Commun.* **2016**, *7*, 13682.

[73] B. Groever, W. T. Chen, F. Capasso, *Nano Lett.* **2017**, *17*, 4902.

[74] S. M. Kamali, A. Arbabi, E. Arbabi, Y. Horie, A. Faraon, *Nat. Commun.* **2016**, *7*, 11618.

[75] W. T. Chen, A. Y. Zhu, M. Khorasaninejad, Z. Shi, V. Sanjeev, F. Capasso, *Nano Lett.* **2017**, *17*, 3188.

[76] F. Aieta, M. A. Kats, P. Genevet, F. Capasso, *Science* **2015**, *347*, 1342.

[77] M. L. Tseng, H. H. Hsiao, C. H. Chu, M. G. Chen, G. Sun, A. Q. Liu, D. P. Tsai, *Adv. Opt. Mater.* **2018**, *6*, 1800554.

[78] S. Wang, P. C. Wu, V. C. Su, Y. C. Lai, C. H. Chu, J. W. Chen, S. H. Lu, J. Chen, B. Xu, C. H. Kuan, T. Li, S. Zhu, D. P. Tsai, *Nat. Commun.* **2017**, *8*, 187.

[79] O. Avayu, E. Almeida, Y. Prior, T. Ellenbogen, *Nat. Commun.* **2017**, *8*, 14992.

[80] D. Lin, A. L. Holsteen, E. Maguid, G. Wetzstein, P. G. Kik, E. Hasman, M. L. Brongersma, *Nano Lett.* **2016**, *16*, 7671.

[81] A. Arbabi, Y. Horie, M. Bagheri, A. Faraon, *Nat. Nanotechnol.* **2015**, *10*, 937.

[82] A. Arbabi, Y. Horie, A. J. Ball, M. Bagheri, A. Faraon, *Nat. Commun.* **2015**, *6*, 7069.

[83] E. Arbabi, A. Arbabi, S. M. Kamali, Y. Horie, A. Faraon, *Sci. Rep.* **2016**, *6*, 32803.

[84] E. Arbabi, A. Arbabi, S. M. Kamali, Y. Horie, A. Faraon, *Optica* **2016**, *3*, 628.

[85] K. Li, Y. Guo, M. Pu, X. Li, X. Ma, Z. Zhao, X. Luo, *Opt. Express* **2017**, *25*, 21419.

[86] M. Khorasaninejad, F. Aieta, P. Kanhaiya, M. A. Kats, P. Genevet, D. Rousso, F. Capasso, *Nano Lett.* **2015**, *15*, 5358.

[87] E. Arbabi, A. Arbabi, S. M. Kamali, Y. Horie, A. Faraon, *Opt. Express* **2016**, *24*, 18468.

[88] E. Arbabi, J. Li, R. J. Hutchins, S. M. Kamali, A. Arbabi, Y. Horie, P. V. Dorpe, V. Gradinaru, D. A. Wagenaar, A. Faraon, *Nano Lett.* **2018**, *18*, 4943.

[89] O. Eisenbach, O. Avayu, R. Ditcovski, T. Ellenbogen, *Opt. Express* **2015**, *23*, 3928.

[90] P. Wang, N. Mohammad, R. Menon, *Sci. Rep.* **2016**, *6*, 21545.

[91] J. Hu, C. Liu, X. Ren, L. J. Lauhon, T. W. Odom, *ACS Nano* **2016**, *10*, 10275.

[92] M. D. Huntington, L. J. Lauhon, T. W. Odom, *Nano Lett.* **2014**, *14*, 7195.

[93] Z. Zhao, M. Pu, H. Gao, J. Jin, X. Li, X. Ma, Y. Wang, P. Gao, X. Luo, *Sci. Rep.* **2015**, *5*, 15781.

[94] M. Khorasaninejad, Z. Shi, A. Y. Zhu, W. T. Chen, V. Sanjeev, A. Zaidi, F. Capasso, *Nano Lett.* **2017**, *17*, 1819.

[95] E. Arbabi, A. Arbabi, S. M. Kamali, Y. Horie, A. Faraon, *Optica* **2017**, *4*, 625.

[96] H. H. Hsiao, Y. H. Chen, R. J. Lin, P. C. Wu, S. Wang, B. H. Chen, D. P. Tsai, *Adv. Opt. Mater.* **2018**, *6*, 1800031.

[97] S. Wang, P. C. Wu, V. C. Su, Y. C. Lai, M. K. Chen, H. Y. Kuo, B. H. Chen, Y. H. Chen, T. T. Huang, J. H. Wang, R. M. Lin, C. H. Kuan, T. Li, Z. Wang, S. Zhu, D. P. Tsai, *Nat. Nanotechnol.* **2018**, *13*, 227.

[98] H. Zhou, L. Chen, F. Shen, K. Guo, Z. Guo, *Phys. Rev. Appl.* **2019**, *11*, 024066.

[99] R. J. Lin, V. C. Su, S. Wang, M. K. Chen, T. L. Chung, Y. H. Chen, H. Y. Kuo, J. W. Chen, J. Chen, Y. T. Huang, J. H. Wang, C. H. Chu, P. C. Wu, T. Li, Z. Wang, S. Zhu, D. P. Tsai, *Nat. Nanotechnol.* **2019**, *14*, 227.

[100] W. T. Chen, A. Y. Zhu, V. Sanjeev, M. Khorasaninejad, Z. Shi, E. Lee, F. Capasso, *Nat. Nanotechnol.* **2018**, *13*, 220.

[101] S. Shrestha, A. C. Overvig, M. Lu, A. Stein, N. Yu, *Light: Sci. Appl.* **2018**, *7*, 85.

[102] W. T. Chen, A. Y. Zhu, J. Sisler, Z. Bharwani, F. Capasso, *Nat. Commun.* **2019**, *10*, 335.

[103] W. T. Chen, A. Y. Zhu, J. Sisler, Y. Huang, K. M. A. Yousef, E. Lee, C. Qiu, F. Capasso, *Nano Lett.* **2018**, *18*, 7801.

[104] M. Khorasaninejad, W. T. Chen, J. Oh, F. Capasso, *Nano Lett.* **2016**, *16*, 3732.

[105] A. Y. Zhu, W. T. Chen, J. Sisler, K. M. A. Yousef, E. Lee, Y.-W. Huang, C.-W. Qiu, F. Capasso, *Adv. Opt. Mater.* **2019**, *7*, 1801144.

[106] M. Faraji-Dana, E. Arbabi, A. Arbabi, S. M. Kamali, H. Kwon, A. Faraon, *Nat. Commun.* **2018**, *9*, 4196.

[107] H. Pahlevaninezhad, M. Khorasaninejad, Y. Huang, Z. Shi, L. P. Hariri, D. C. Adams, V. Ding, A. Zhu, C. Qiu, F. Capasso, M. J. Suter, *Nat. Photonics* **2018**, *12*, 540.

[108] B. H. Chen, P. C. Wu, V. C. Su, Y. C. Lai, C. H. Chu, I. C. Lee, J. W. Chen, Y. H. Chen, Y. C. Lan, C. H. Kuan, D. P. Tsai, *Nano Lett.* **2017**, *17*, 6345.

[109] X. Li, L. Chen, Y. Li, X. Zhang, M. Pu, Z. Zhao, X. Ma, Y. Wang, M. Hong, X. Luo, *Sci. Adv.* **2016**, *2*, e1601102.

[110] B. Wang, F. Dong, Q. Li, D. Yang, C. Sun, J. Chen, Z. Song, L. Xu, W. Chu, Y. Xiao, Q. Gong, Y. Li, *Nano Lett.* **2016**, *16*, 5235.

[111] Z. Jin, S. Mei, S. Chen, Y. Li, C. Zhang, Y. He, X. Yu, C. Yu, J. K. W. Yang, B. Luk'yanchuk, S. Xiao, C. W. Qiu, *ACS Nano* **2019**, *13*, 821.